Electronic Supplementary Information for:

Hydroboration of CO_2 catalyzed by bis(phosphinite) pincer ligated nickel thiolate complexes

Ting Liu, Wenjuan Meng, Qiang-Qiang Ma, Jie Zhang,* Huizhen Li, Shujun Li, Qianyi Zhao and Xuenian Chen*

School of Chemistry and Chemical Engineering, Henan Key Laboratory of Boron Chemistry and Advanced Energy Materials, Henan Normal University, Xinxiang, Henan 453007, China

E-mails: jie.zhang@htu.edu.cn (J.Z.); xnchen@htu.edu.cn (X.C.)

Experimental details for syntheses, characterization and catalytic reactions

General Information. Unless otherwise indicated, all the syntheses were carried out under a nitrogen atmosphere using standard Schlenk and glove box techniques. Solvents used for the reactions were degassed and dried using standard procedures. Benzene-d_6 was distilled from Na and benzophenone under nitrogen atmosphere. Catecholborane was purchased from Sigma-Aldrich and purified by vacuum distillation. NMR spectra were recorded on a Bruker Advance 400 MHz or a Bruker AVANCE III 600 MHz spectrometer. Mass spectra were performed on a Bruker micrOTOF II instrument. The starting nickel chloride complexes [2,6-$(R_2PO)_2C_6H_3$]NiCl (R = ^{t}Bu, ^{i}Pr)[1,2] and the thiolate complexes **3a**-**d**[3] were synthesized according to published procedures.

Synthesis of [2,6-(^{t}Bu$_2$PO)$_2$C$_6$H$_3$]NiSC$_6$H$_4$-*p*-OCH$_3$ (1a). To a suspension of NaH (120 mg, 5.0 mmol) in 40 mL of THF was added 4-methoxybenzenethiol (701 mg, 5.0 mmol) at 0 ℃ under a nitrogen atmosphere. The resulting mixture was warmed to room temperature and stirred for 1 h. Then, [2,6-(^{t}Bu$_2$PO)$_2$C$_6$H$_3$]NiCl (492 mg, 1 mmol) was added, and the mixture was refluxed for 24 h. After cooling to room temperature, the volatiles were removed under vacuum and the residue was extracted with toluene and filtered through a pad of Celite. Removal of toluene under vacuum followed by recrystallization in hexane produced complex **1a** as a red crystalline solid (447 mg, 75% yield). ^{1}H NMR (400 MHz, $CDCl_3$, δ): 7.37 (d, 2H, Ar*H*, J = 8.8 Hz), 6.94 (t, 1H, Ar*H*, J = 7.9 Hz), 6.63 (d, 2H, Ar*H*, J = 8.8 Hz), 6.42 (d, 2H, Ar*H*, J = 7.9 Hz), 3.73 (s, 3H, OCH_3), 1.38–1.41 (m, 36H, C(CH_3)$_3$). ^{13}C{^{1}H} NMR (101 MHz, $CDCl_3$, δ): 168.9 (t, Ar*C*, $J_{C\text{-}P}$ = 9.1 Hz), 156.7 (s, Ar*C*), 136.6 (t, Ar*C*, $J_{C\text{-}P}$ = 5.5 Hz), 135.5 (s, Ar*C*), 128.8 (t, Ar*C*, $J_{C\text{-}P}$ = 19.6 Hz), 128.4 (s, Ar*C*), 114.0 (s, Ar*C*), 104.4 (t, Ar*C*, $J_{C\text{-}P}$ = 6.1 Hz), 55.6 (s, OCH_3), 39.9 (t, *C*(CH$_3$)$_3$, $J_{C\text{-}P}$ = 7.4 Hz), 28.3 (t, C(*C*H$_3$)$_3$, $J_{C\text{-}P}$ = 2.8 Hz). ^{31}P{^{1}H} NMR (162 MHz, $CDCl_3$, δ): 187.6 (s). Anal. Calcd for $C_{29}H_{46}NiO_3P_2S$: C, 58.50; H, 7.79. Found: C, 58.28; H, 7.54.

Synthesis of [2,6-(^{t}Bu$_2$PO)$_2$C$_6$H$_3$]NiSC$_6$H$_4$-*p*-CH$_3$ (1b). Complex **1b** was prepared in 83% yield as a red crystalline solid by a procedure similar to that used for **1a.** ^{1}H NMR (400 MHz, $CDCl_3$, δ): 7.36 (d, 2H, Ar*H*, J = 7.9 Hz), 6.94 (t, 1H, Ar*H*, J = 7.9 Hz), 6.83 (d, 2H, Ar*H*, J = 7.9 Hz), 6.42 (d, 2H, Ar*H*, J = 7.9 Hz), 2.21 (s, 3H, CH_3), 1.38–1.41 (m, 36H, C(CH_3)$_3$). ^{13}C{^{1}H} NMR (101 MHz, $CDCl_3$, δ): 168.9 (t, Ar*C*, $J_{C\text{-}P}$ = 9.0 Hz), 142.3 (t, Ar*C*, $J_{C\text{-}P}$ = 4.5 Hz), 134.5 (s, Ar*C*), 132.3 (s, Ar*C*), 128.8 (t, Ar*C*, $J_{C\text{-}P}$ = 20.3 Hz), 128.7 (s, Ar*C*), 128.4 (s, Ar*C*), 104.4 (t, Ar*C*, $J_{C\text{-}P}$ = 5.8 Hz), 39.9 (t,

C(CH_3)$_3$, J_{C-P} = 7.4 Hz), 28.4 (t, C(*C*H$_3$)$_3$, J_{C-P} = 2.8 Hz), 21.0 (s, *C*H$_3$). $^{31}P\{^1H\}$ NMR (162 MHz, C_6D_6, δ): 187.4 (s). Anal. Calcd for $C_{29}H_{46}NiO_2P_2S$: C, 60.12; H, 8.00. Found: C, 60.24; H, 8.11.

Synthesis of [2,6-(^{t}Bu$_2$PO)$_2$C$_6$H$_3$]NiSPh (1c). Complex 1c was prepared in 81% yield as an orange crystalline solid by a procedure similar to that used for **1a**. ^1H NMR (400 MHz, C_6D_6, δ): 7.79 (d, 2H, Ar*H*, *J* = 7.4 Hz), 7.00-7.04 (m, 2H, Ar*H*), 6.91-6.95 (m, 2H, Ar*H*), 6.62 (d, 2H, Ar*H*, *J* = 7.9 Hz), 1.36–1.40 (m, 36H, C(C*H*$_3$)$_3$). $^{13}C\{^1H\}$ NMR (101 MHz, $CDCl_3$, δ): 168.8 (t, Ar*C*, J_{C-P} = 9.1 Hz), 146.5 (t, Ar*C*, J_{C-P} = 4.5 Hz), 134.6 (s, Ar*C*), 128.5 (t, Ar*C*, J_{C-P} = 19.4 Hz), 128.4 (s, Ar*C*), 127.7 (s, Ar*C*), 122.6 (s, Ar*C*), 104.3 (t, Ar*C*, J_{C-P} = 5.9 Hz), 39.8 (t, *C*(CH_3)$_3$, J_{C-P} = 7.4 Hz), 28.2 (t, C(*C*H$_3$)$_3$, J_{C-P} = 2.8 Hz). $^{31}P\{^1H\}$ NMR (162 MHz, C_6D_6, δ): 187.2 (s). HRMS (ESI): m/z Calculated for $C_{28}H_{44}NiO_2P_2S + Na^+$ $[M + Na]^+$ 587.1783, found 587.1760. Anal. Calcd for $C_{28}H_{44}NiO_2P_2S$: C, 59.49; H, 7.84. Found: C, 59.40; H, 7.69.

Synthesis of [2,6-(^{t}Bu$_2$PO)$_2$C$_6$H$_3$]NiSC$_6$H$_4$-*p*-CF$_3$ (1d). Complex **1d** was prepared in 70% yield as a yellow crystalline solid by a procedure similar to that used for **1a**. ^1H NMR (400 MHz, $CDCl_3$, δ): 7.55 (d, 2H, Ar*H*, *J* = 8.0 Hz), 7.23 (d, 2H, Ar*H*, *J* = 8.0 Hz), 6.97 (t, 1H, Ar*H*, *J* = 8.0 Hz), 6.44 (d, 2H, Ar*H*, *J* = 8.0 Hz), 1.38–1.42 (m, 36H, C(C*H*$_3$)$_3$). $^{13}C\{^1H\}$ NMR (101 MHz, $CDCl_3$, δ): 169.0 (t, Ar*C*, J_{C-P} = 9.1 Hz), 153.5 (s, Ar*C*), 134.2 (s, Ar*C*), 128.9 (s, Ar*C*), 128.0 (t, Ar*C*, J_{C-P} = 19.4 Hz), 126.4 (q, *C*F$_3$, J_{C-F} = 110.0 Hz), 124.3 (q, Ar*C*, J_{C-F} = 32.3 Hz), 124.3 (q, Ar*C*, J_{C-F} = 3.6 Hz), 104.6 (t, Ar*C*, J_{C-P} = 5.4 Hz), 39.9 (t, *C*(CH_3)$_3$, J_{C-P} = 7.4 Hz), 28.4 (t, C(*C*H$_3$)$_3$, J_{C-P} = 2.8 Hz). $^{31}P\{^1H\}$ NMR (162 MHz, $CDCl_3$, δ): 187.2 (s). Anal. Calcd for $C_{29}H_{49}F_3NiO_2P_2S$: C, 55.00; H, 6.84. Found: C, 55.08; H, 6.91.

Synthesis of [2,6-(^{t}Bu$_2$PO)$_2$C$_6$H$_3$]NiSCH$_2$Ph (2). To a suspension of NaH (120 mg, 5.0 mmol) in 30 mL of THF was added phenylmethanethiol (621 mg, 5.0 mmol) at 0 ℃ under a nitrogen atmosphere. The resulting mixture was warmed to room temperature and stirred for 1 h. Then, [2,6-(^{t}Bu$_2$PO)$_2$C$_6$H$_3$]NiCl (492 mg, 1 mmol) was added, and the mixture was refluxed for 24 h. After cooling to room temperature, the volatiles were removed under vacuum and the residue was extracted with toluene and filtered through a pad of Celite. Removal of toluene under vacuum followed by recrystallization in hexane produced complex **2** as a dark orange solid (441 mg, 76% yield). ^1H NMR (400 MHz, C_6D_6, δ): 7.57 (d, 2H, Ar*H*, *J* = 7.3 Hz), 7.23 (t, 2H, Ar*H*, *J* = 7.9 Hz), 7.08 (t, 1H, Ar*H*, *J* = 7.5 Hz), 6.93 (t, 1H, Ar*H*, *J* = 7.9 Hz), 6.64 (d, 2H, Ar*H*, *J* = 7.9 Hz), 3.75 (s, 2H, SC*H*$_2$), 1.42–1.45 (m, 36H, C(C*H*$_3$)$_3$). $^{13}C\{^1H\}$ NMR (101 MHz, C_6D_6, δ): 169.1 (t, Ar*C*, J_{C-P} = 9.2 Hz), 145.9 (s, Ar*C*),

131.1 (t, Ar*C*, $J_{C\text{-}P}$ = 20.5 Hz), 128.9 (s, Ar*C*), 128.8 (s, Ar*C*), 128.4 (t, Ar*C*, $J_{C\text{-}P}$ = 11.2 Hz), 126.1 (s, Ar*C*), 104.8 (t, Ar*C*, $J_{C\text{-}P}$ = 5.4 Hz), 39.4 (t, *C*$(CH_3)_3$, $J_{C\text{-}P}$ = 7.5 Hz), 38.1 (t, S*C*H_2, $J_{C\text{-}P}$ = 6.7 Hz), 28.5 (s, C(*C*$H_3)_3$). $^{31}P\{^1H\}$ NMR (162 MHz, C_6D_6, δ): 190.8 (s). HRMS (ESI): m/z Calculated for $C_{29}H_{46}NiO_2P_2S$ + Na^+ $[M + Na]^+$ 601.1939, found 601.1934. Anal. Calcd for $C_{29}H_{46}NiO_2P_2S$: C, 60.12; H, 8.00. Found: C, 60.27; H, 8.06.

Synthesis of [2,6-(^{i}Pr$_2$PO)$_2$C$_6$H$_3$]NiSCH$_2$Ph (4). Complex **4** was prepared from [2,6-(^{i}Pr$_2$PO)$_2$C$_6$H$_3$]NiCl, phenylmethanethiol and NaH in 86% yield by procedure similar to that used for **2**. ^1H NMR (400 MHz, C_6D_6, δ): 7.57 (d, 2H, Ar*H*, *J* = 7.4 Hz), 7.23 (t, 2H, Ar*H*, *J* = 7.9 Hz), 7.09 (t, 1H, Ar*H*, *J* = 7.5 Hz), 6.92 (t, 1H, Ar*H*, *J* = 7.9 Hz), 6.69 (d, 2H, Ar*H*, *J* = 7.9 Hz), 3.76 (s, 2H, SC*H*$_2$), 2.10-2.17 (m, 4H, C*H*$(CH_3)_2$), 1.13–1.37 (m, 24H, CH(C*H*$_3)_2$). $^{13}C\{^1H\}$ NMR (101 MHz, C_6D_6, δ): 168.4 (t, Ar*C*, $J_{C\text{-}P}$ = 9.7 Hz), 146.2 (s, Ar*C*), 133.1 (t, Ar*C*, $J_{C\text{-}P}$ = 20.7 Hz), 129.0 (s, Ar*C*), 128.8 (s, Ar*C*), 128.4 (t, Ar*C*, $J_{C\text{-}P}$ = 13.3 Hz), 126.2 (s, Ar*C*), 105.2 (t, Ar*C*, $J_{C\text{-}P}$ = 5.9 Hz), 37.7 (t, S*C*H_2, $J_{C\text{-}P}$ = 10.9 Hz), 29.1 (t, *C*H$(CH_3)_2$, $J_{C\text{-}P}$ = 12.0 Hz), 17.8 (s, CH(*C*$H_3)_2$), 16.9 (s, CH(*C*$H_3)_2$). $^{31}P\{^1H\}$ NMR (162 MHz, C_6D_6, δ): 191.9 (s). HRMS (ESI): m/z Calculated for $C_{25}H_{38}NiO_2P_2S$ + Na^+ $[M + Na]^+$ 545.1313, found 545.1334. Anal. Calcd for $C_{25}H_{38}NiO_2P_2S$: C, 57.38; H, 7.32. Found: C, 57.37; H, 7.25.

Multinuclear NMR Characterization of [2,6-(^{i}Pr$_2$PO)$_2$C$_6$H$_3$]NiB(cat)$_2$ (6). Complex **6** was isolated from the reaction mixture of **3c** catalyzed hydroboration of CO_2 as light yellow crystals and was characterized by multinuclear NMR. ^1H NMR (400 MHz, C_6D_6, δ): 7.11–7.13 (m, 4H, Ar*H*), 6.79–6.81 (m, 4H, Ar*H*), 6.76 (t, 1H, Ar*H*, *J* = 8.1 Hz), 6.38 (d, 2H, Ar*H*, *J* = 8.1 Hz), 2.30–2.37 (m, 4H, C*H*$(CH_3)_2$), 0.97–1.11 (m, 24H, CH(C*H*$_3)_2$). $^{13}C\{^1H\}$ NMR (101 MHz, C_6D_6, δ): 169.7 (t, Ar*C*, $J_{C\text{-}P}$ = 9.7 Hz), 151.0 (s, Ar*C*), 130.8 (t, Ar*C*, $J_{C\text{-}P}$ = 34.0 Hz), 128.6 (s, Ar*C*), 128.5 (s, Ar*C*), 119.8 (s, Ar*C*), 110.6 (s, Ar*C*), 106.1 (t, Ar*C*, $J_{C\text{-}P}$ = 6.0 Hz), 28.3 (t, *C*H$(CH_3)_2$, $J_{C\text{-}P}$ = 10.3 Hz), 16.9 (s, CH(*C*$H_3)_2$), 16.0 (s, CH(*C*$H_3)_2$). $^{31}P\{^1H\}$ NMR (162 MHz, C_6D_6, δ): 179.9 (s). ^{11}B NMR (128 MHz, C_6D_6, δ): 14.4 (s).

X-ray Structure Determination. Single crystals of complexes **1a-d** were obtained from recrystallization in CH_2Cl_2/*n*-hexane; single crystals of complexes **2** and **4** were obtained from recrystallization in pure *n*-hexane; single crystals of complex **6** were obtained from the catalytic reaction mixture. Intensity data were collected at 100 K for complex **1a**, 103 K for complexes **2** and **4**, 153 K for complex **1c** and 296 K for complexes **1b** and **1d** on a Bruker SMART6000 CCD

diffractometer using graphite-monochromated Mo Kα radiation (λ = 0.71073 Å). Intensity data were collected at 293 K for complex **6** on a SuperNova diffractometer (Oxford Diffraction) with graphite-monochromatized Mo Kα radiation (λ = 0.71073 Å). The frames were integrated with the Bruker APEX2 software package using a narrow-frame algorithm. The data were corrected for decay, Lorentz, and polarization effects as well as absorption and beam corrections based on the multi-scan technique. The structures were solved by a combination of direct methods in SHELXTL and the difference Fourier technique and refined by full-matrix least-squares procedures. Nonhydrogen atoms were refined with anisotropic displacement parameters. The H-atoms were either located or calculated and subsequently treated with a riding model. Complex **1a** crystallized as three independent molecules in the crystalline lattice; complex **4** crystallized as two independent molecules in the crystalline lattice and disorder was observed for the phenylmethanethiolate group in one molecule of **4**. Disorder was also observed for the CF_3 group in the molecule of **1d**. No solvent of crystallization was present in the lattice for any of the structures.

General Procedure for Catalytic Hydroboration of CO_2. Catalytic hydroboration of CO_2 was carried out at room temperature under 1 atm of CO_2 in benzene or benzene-d_6 with a catalyst to substrate ratio of 1:500. Typically, 0.011 mmol of the nickel thiolate complex, 5.50 mmol of HBcat, 0.022 mmol of hexamethylbenzene (as an internal standard) and 4 mL of benzene or benzene-d_6 were mixed in a flame-dried 50 mL Schlenk flask under a nitrogen atmosphere. Then CO_2 was bubbled through the solution until the temperature of the reaction mixture increased from 25 ˚C to 40-45 ˚C and a large amount of white precipitate developed. The mixture was stirred for an additional 2 min and cooled to room temperature. The resulting white precipitate was allowed to settle, and then 0.6 mL of the clear liquid was transferred under nitrogen into a NMR tube. ^{11}B NMR and ^{1}H NMR spectra were recorded.[4] Turnover numbers (TONs) were calculated based on B−H bond by comparing the ^{1}H NMR integration of the CH_3OBcat methyl resonance (3.36 ppm) with that of the internal standard (2.11 ppm).

Reference

1. S. Chakraborty, J. A. Krause and H. Guan, *Organometallics*, 2009, **28**, 582.
2. V. Pandarus and D. Zargarian, *Organometallics*, 2007, **26**, 4321.
3. J. Zhang, A. Adhikary, K. M. King, J. A. Krause and H. Guan, *Dalton Trans.*, 2012, **41**, 7959.
4. When benzene was used as the solvent ^{1}H NMR spectra were recorded after mixing 0.3 mL of the clear solution with 0.3 mL of benzene-d_6 in a NMR tube under a nitrogen atmosphere.

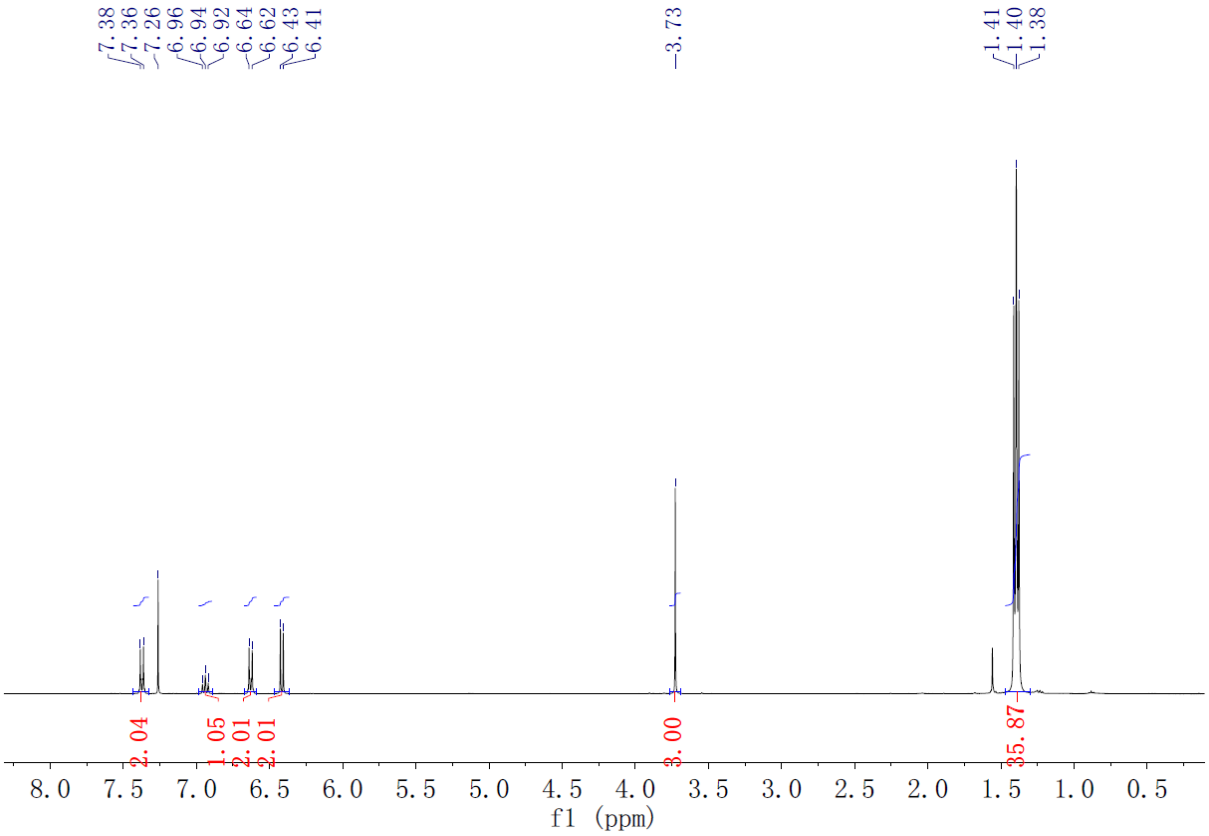

Figure S1 ^{1}H NMR spectrum of **1a** ($CDCl_3$)

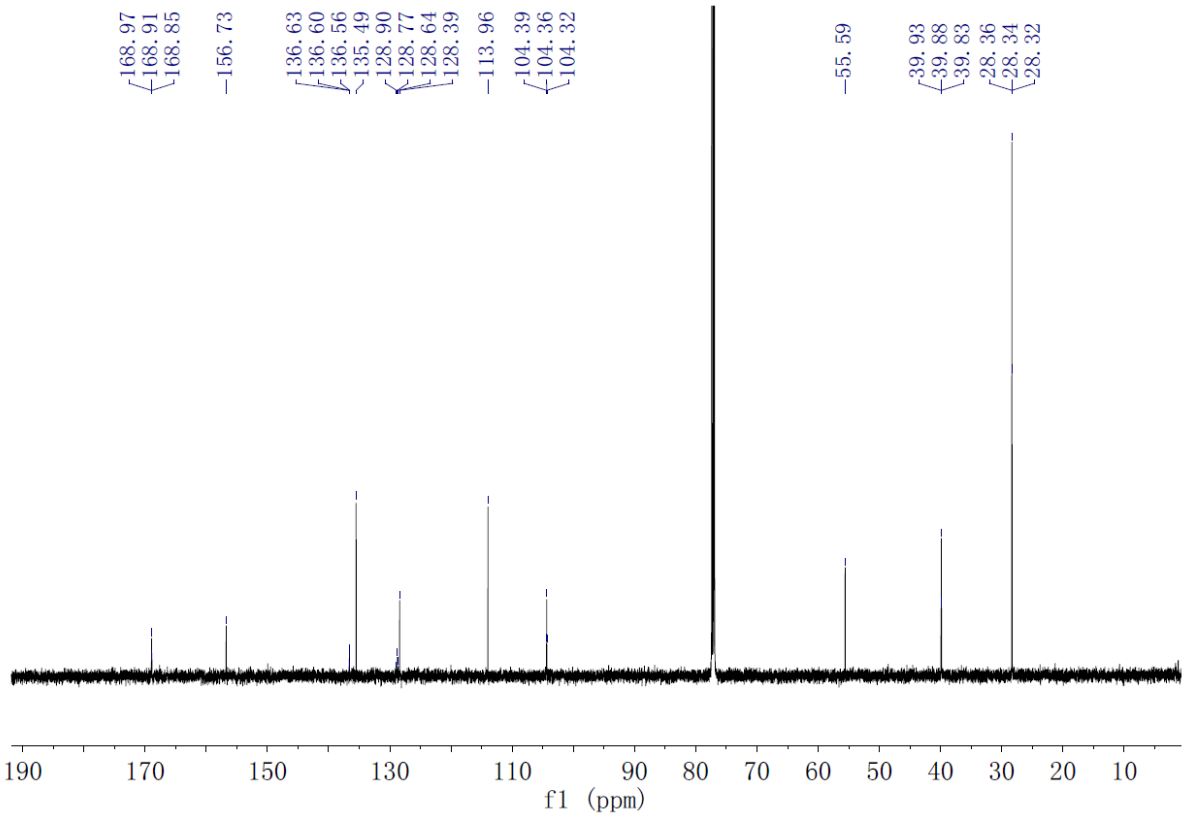

Figure S2 $^{13}C\{^{1}H\}$ NMR spectrum of **1a** ($CDCl_3$)

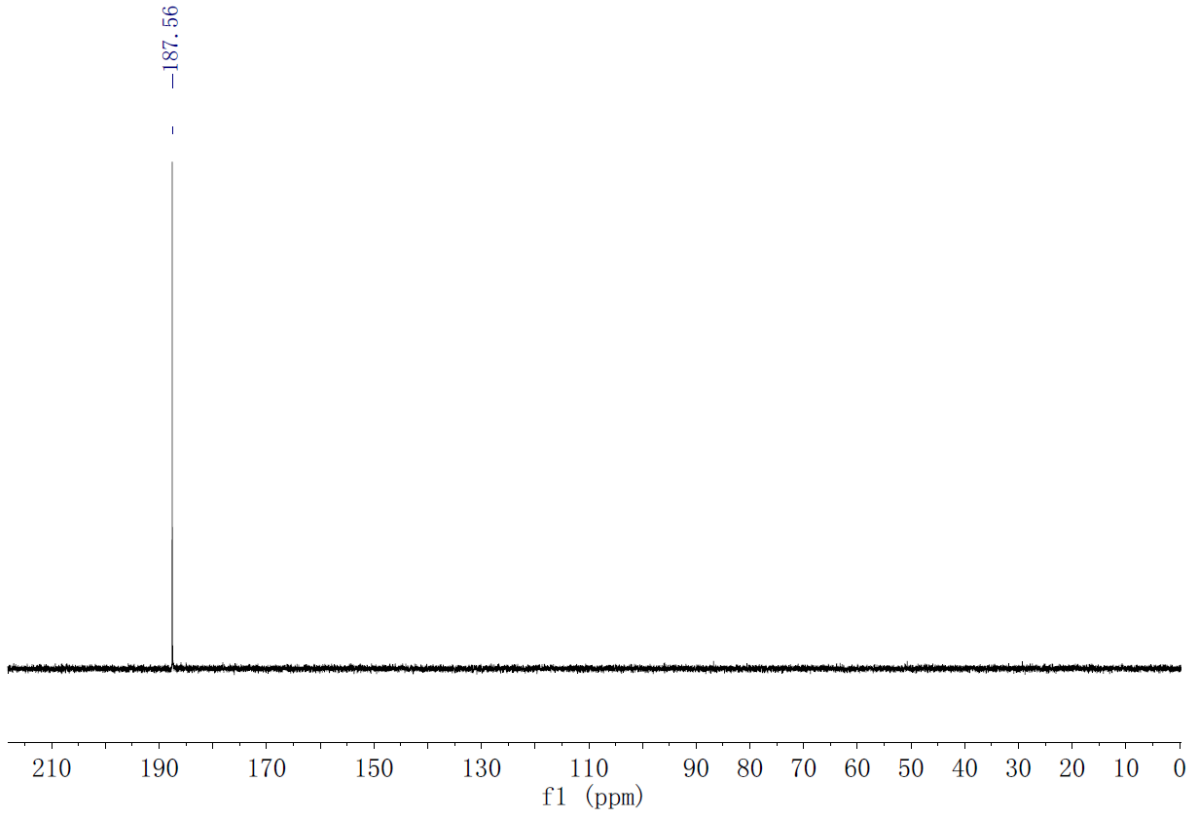

Figure S3 $^{31}P\{^{1}H\}$ NMR spectrum of **1a** ($CDCl_3$)

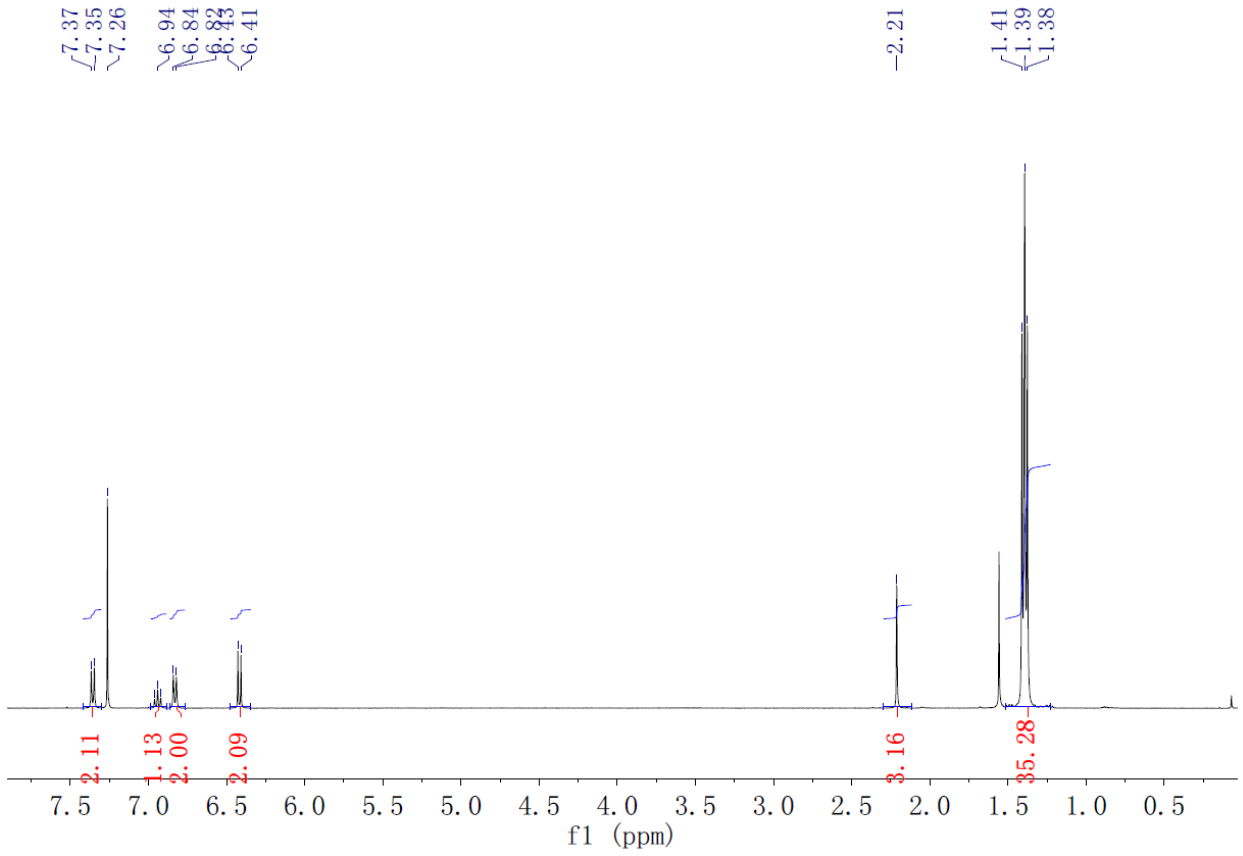

Figure S4 ^{1}H NMR spectrum of **1b** ($CDCl_3$)

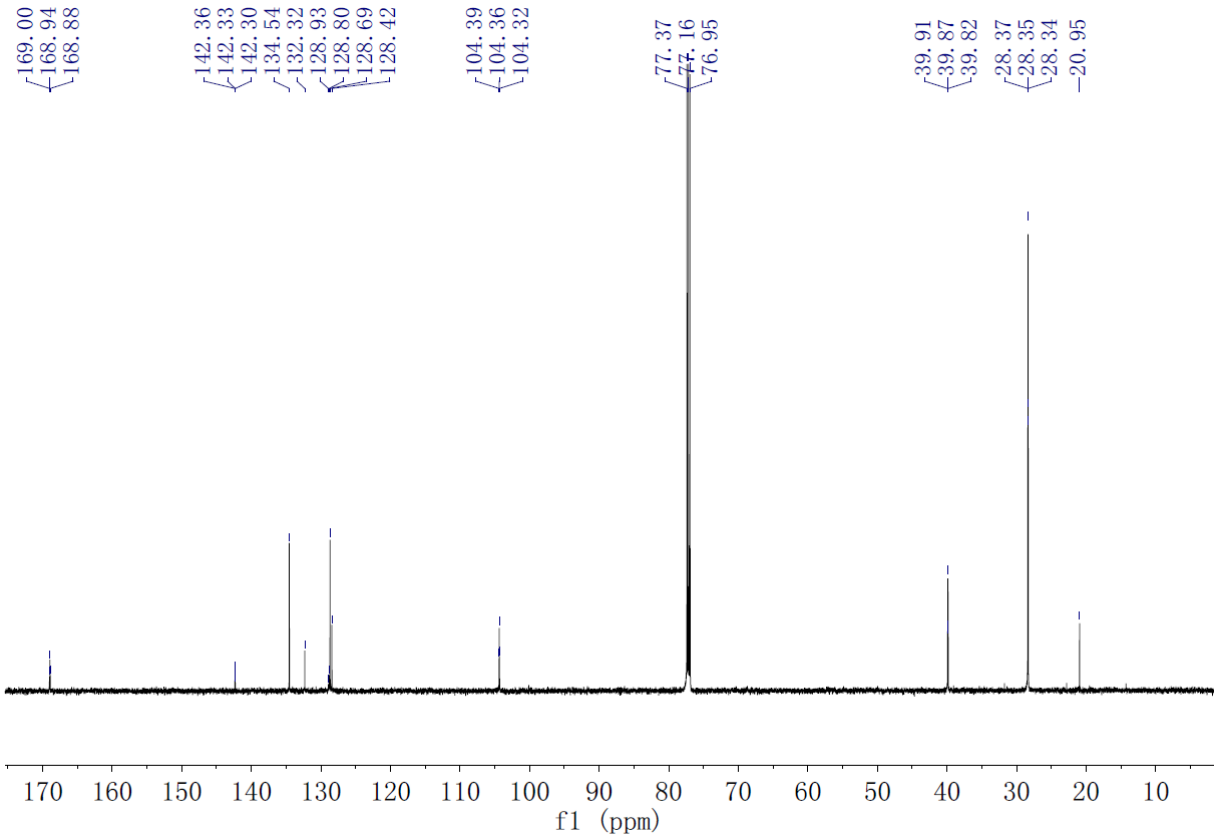

Figure S5 $^{13}C\{^{1}H\}$ NMR spectrum of **1b** ($CDCl_3$)

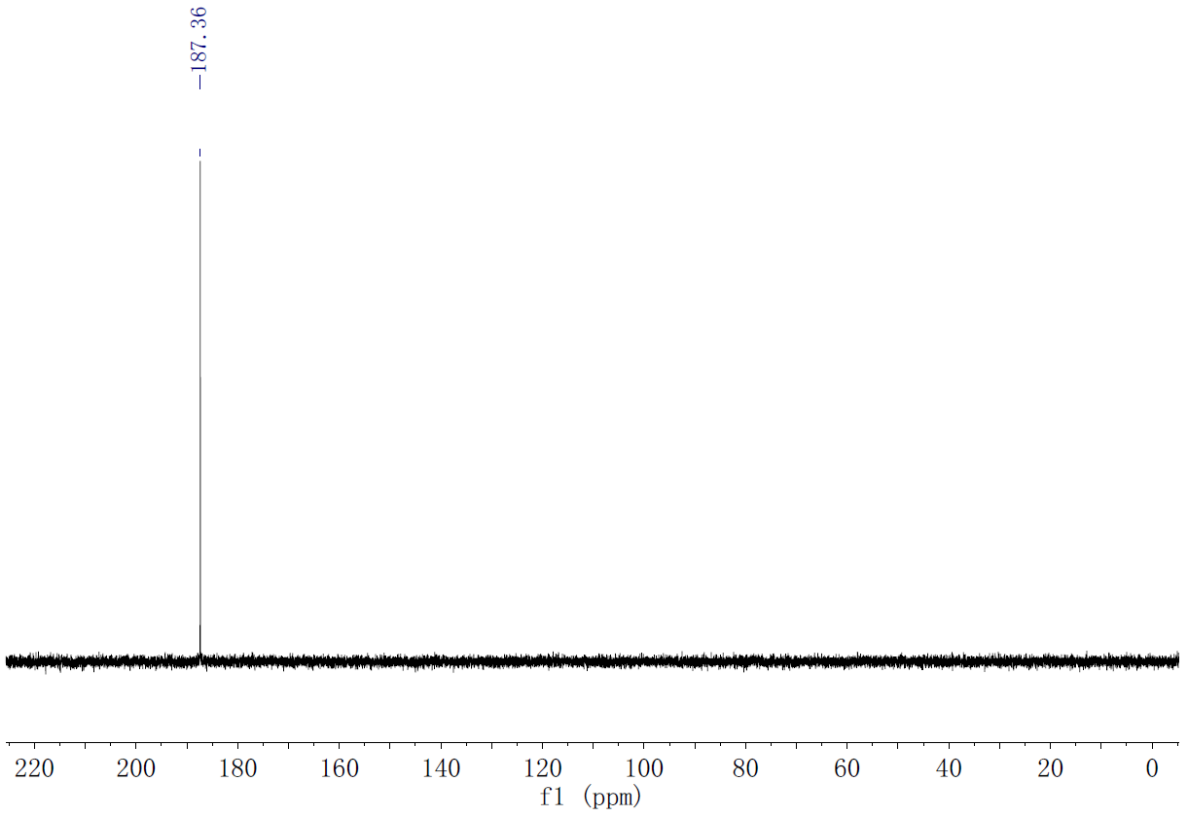

Figure S6 $^{31}P\{^{1}H\}$ NMR spectrum of **1b** (benzene-d_6)

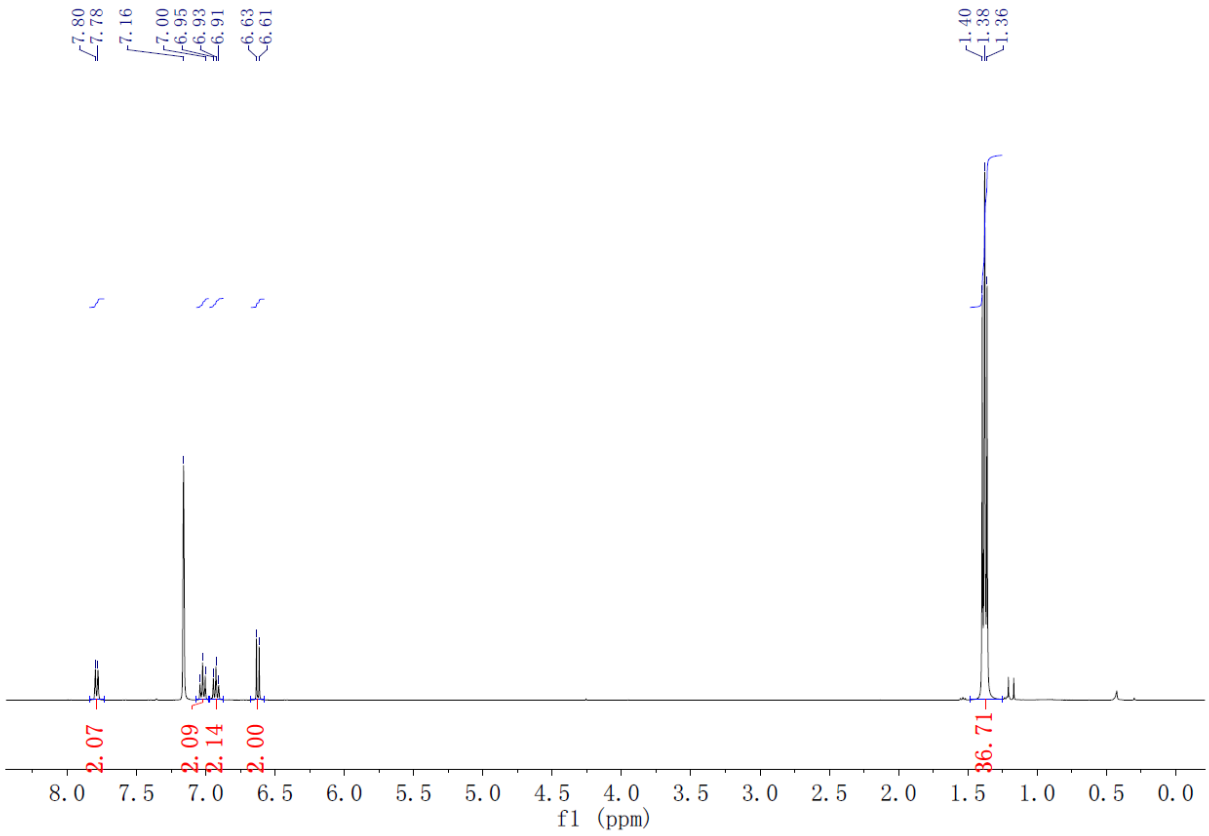

Figure S7 ^{1}H NMR spectrum of **1c** (benzene-d_6)

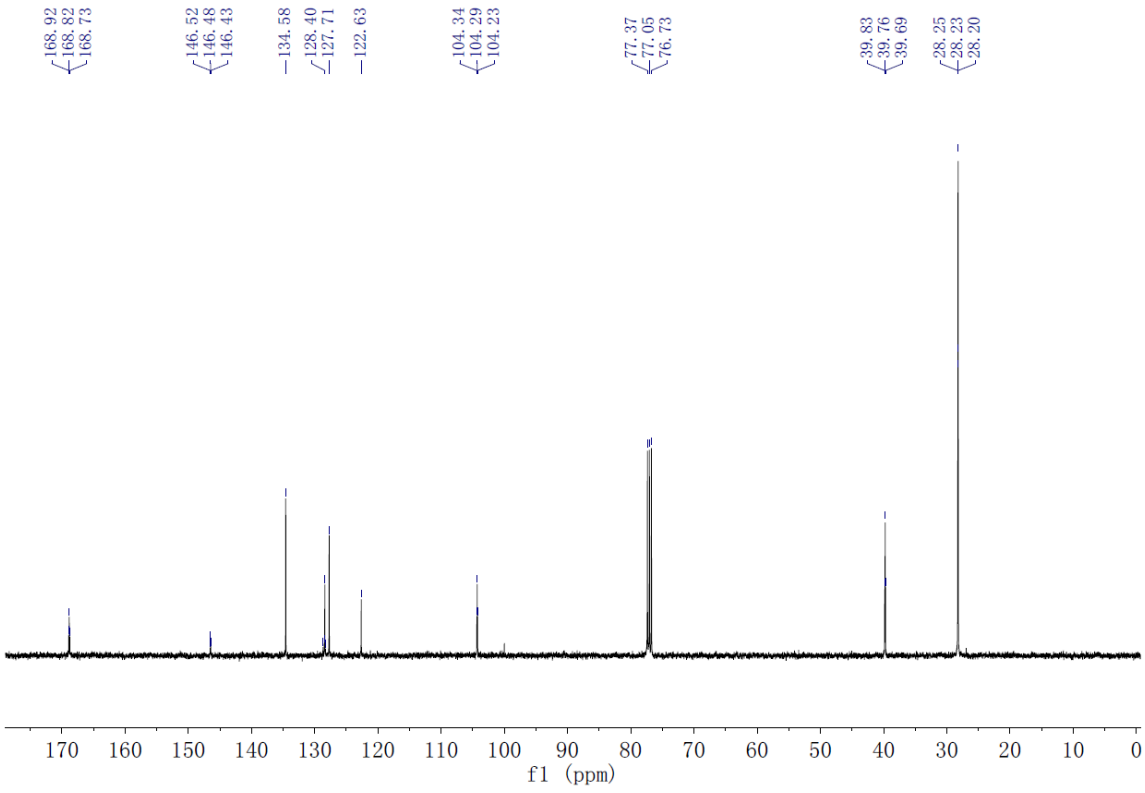

Figure S8 ^{13}C{^{1}H} NMR spectrum of **1c** ($CDCl_3$)

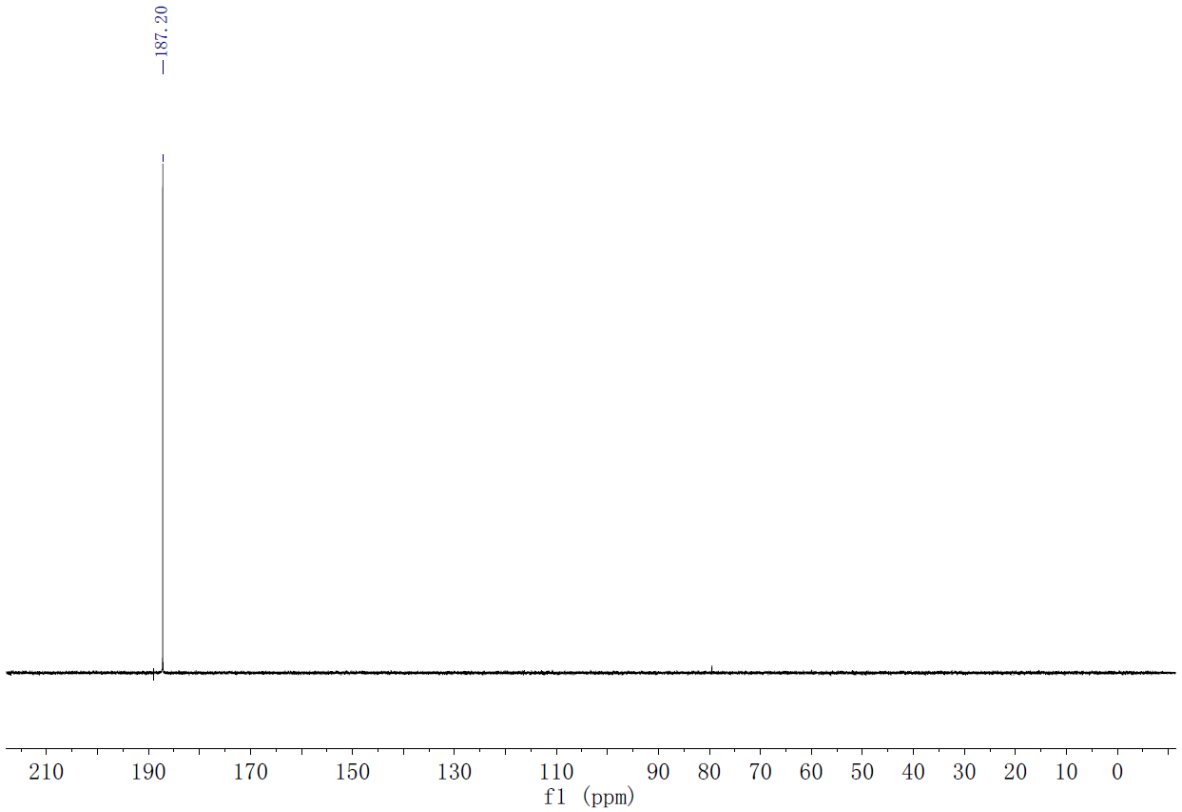

Figure S9 $^{31}P\{^{1}H\}$ NMR spectrum of **1c** (benzene-d_6)

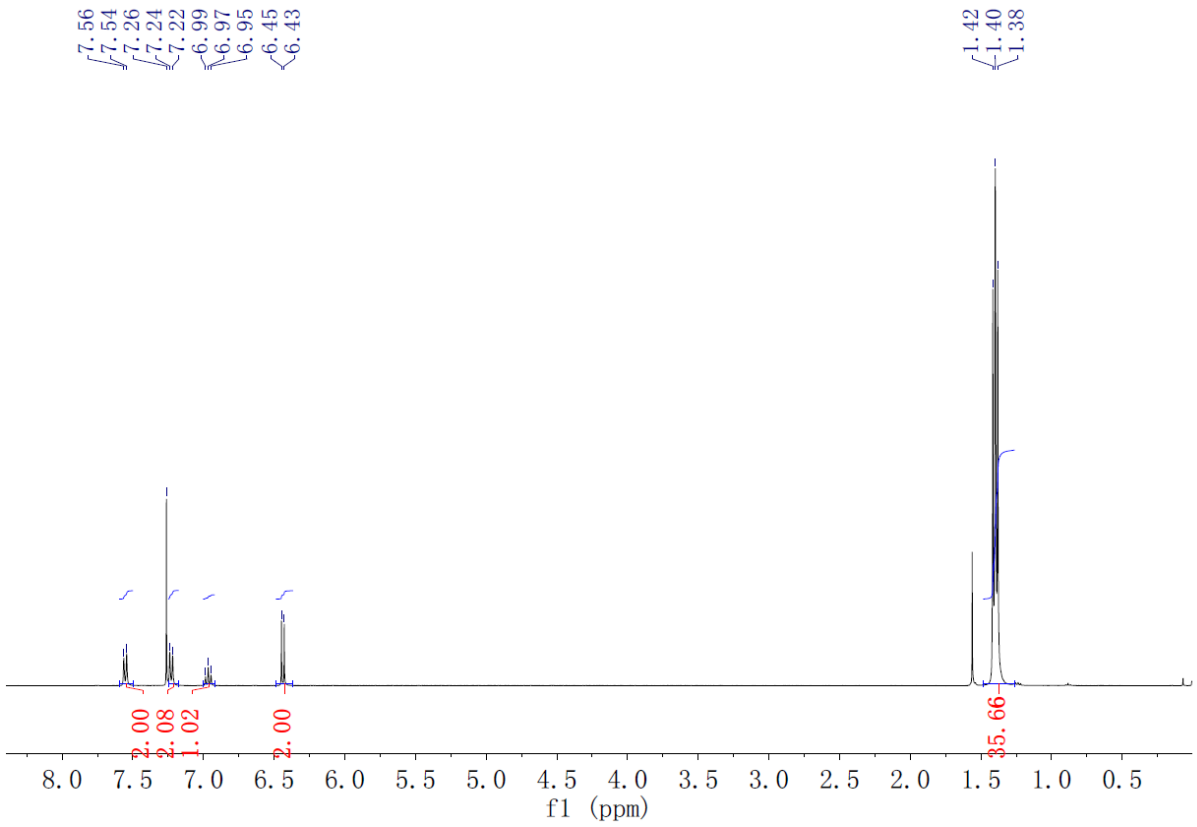

Figure S10 ^{1}H NMR spectrum of **1d** ($CDCl_3$)

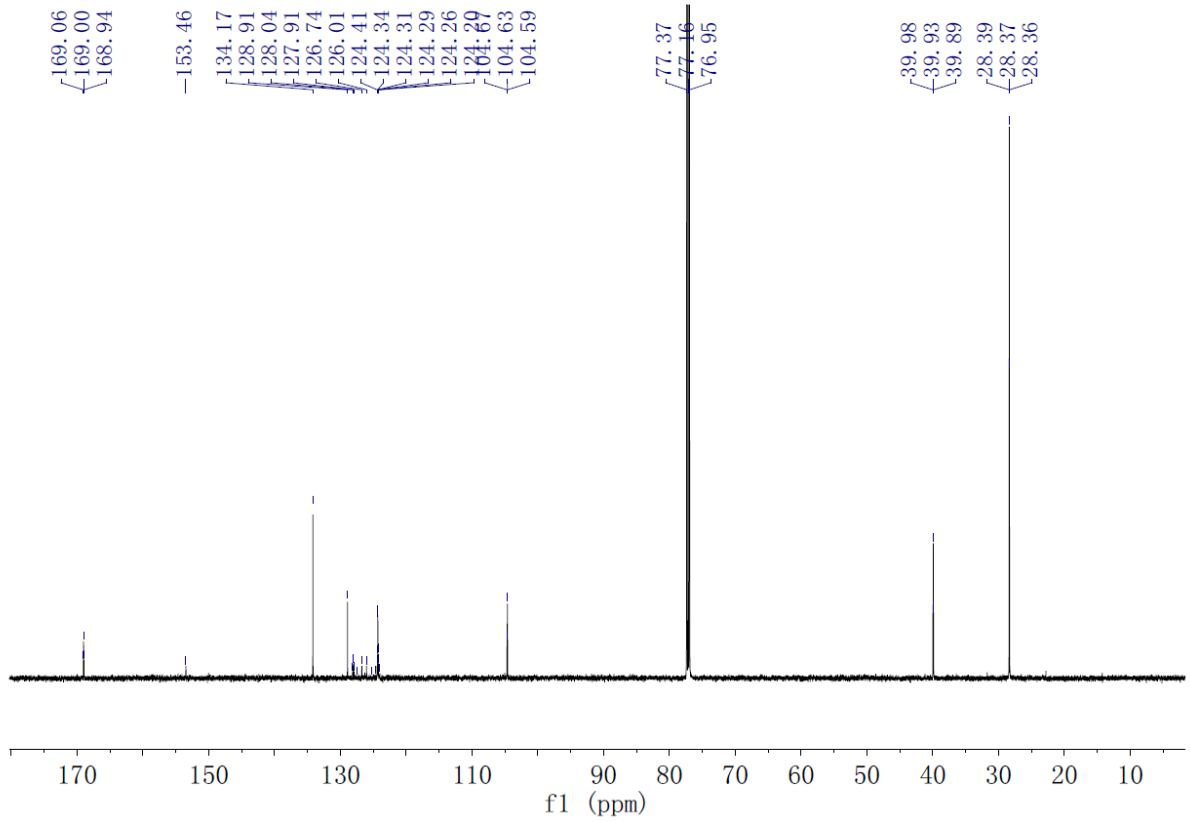

Figure S11 $^{13}C\{^{1}H\}$ NMR spectrum of **1d** ($CDCl_3$)

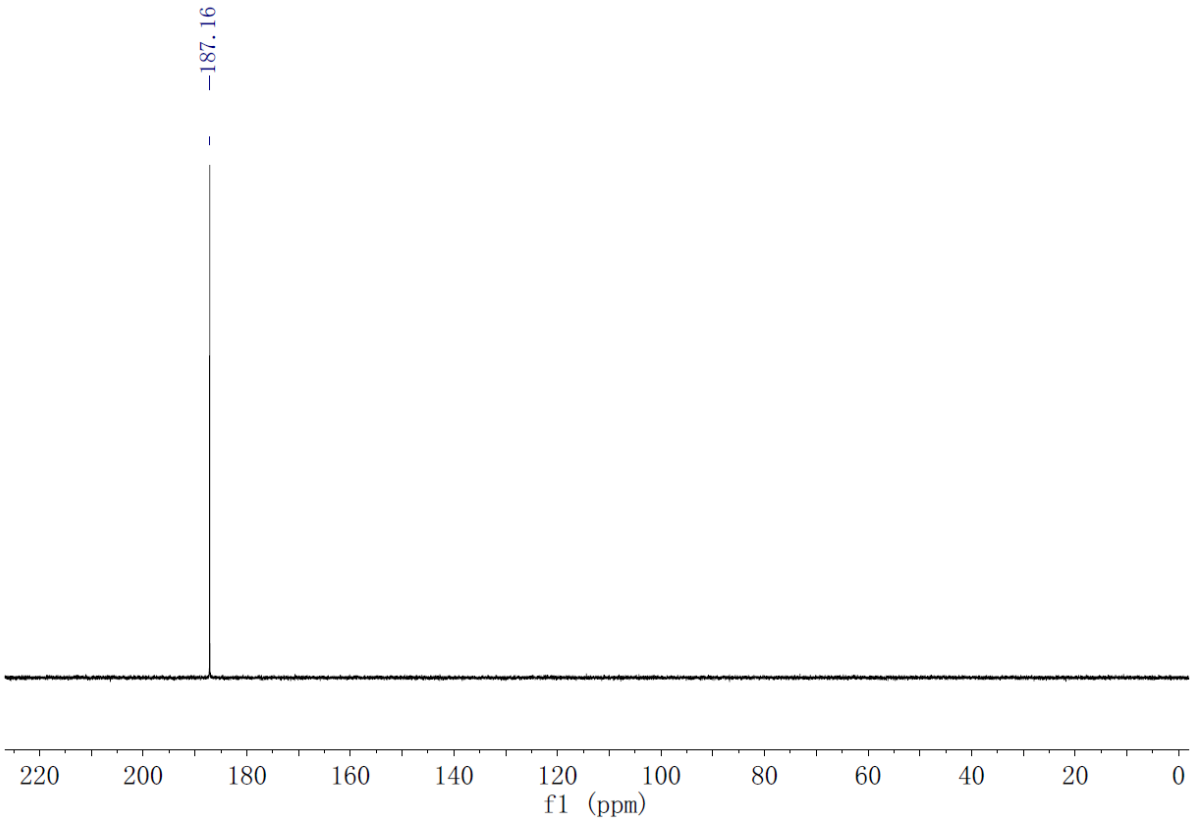

Figure S12 $^{31}P\{^{1}H\}$ NMR spectrum of **1d** ($CDCl_3$)

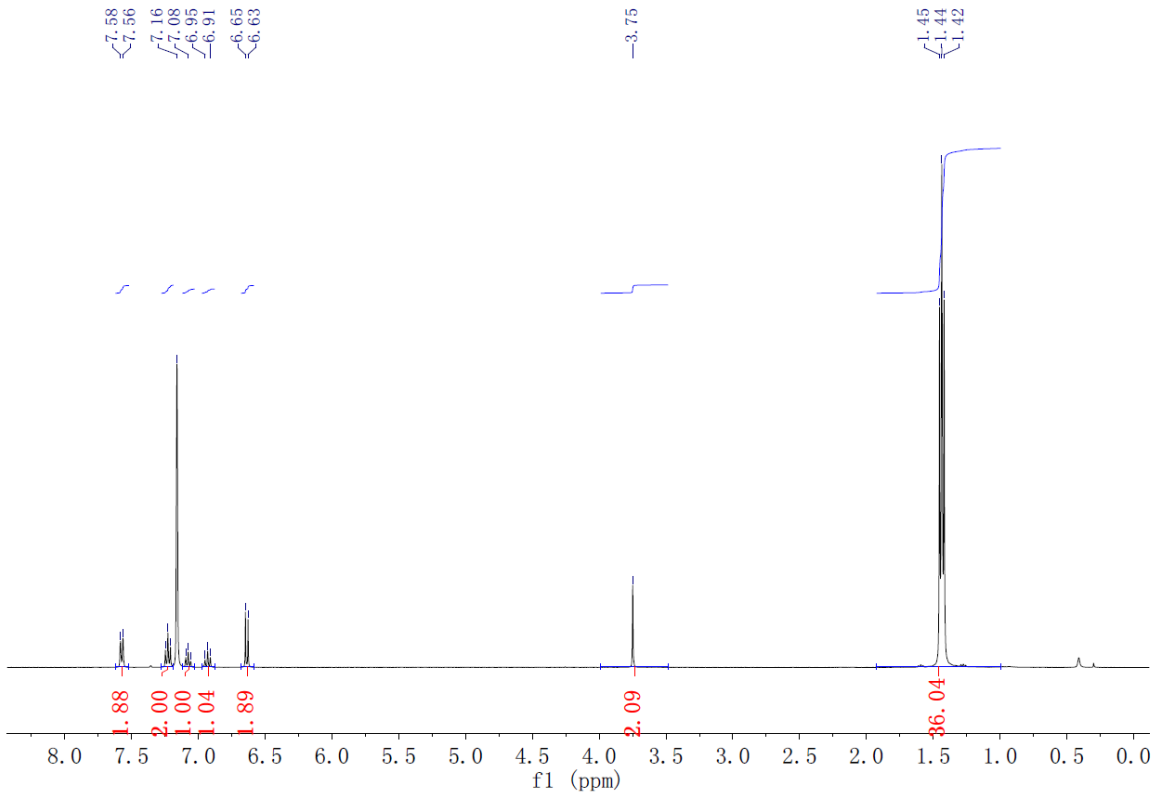

Figure S13 ^{1}H NMR spectrum of **2** (benzene-d_6)

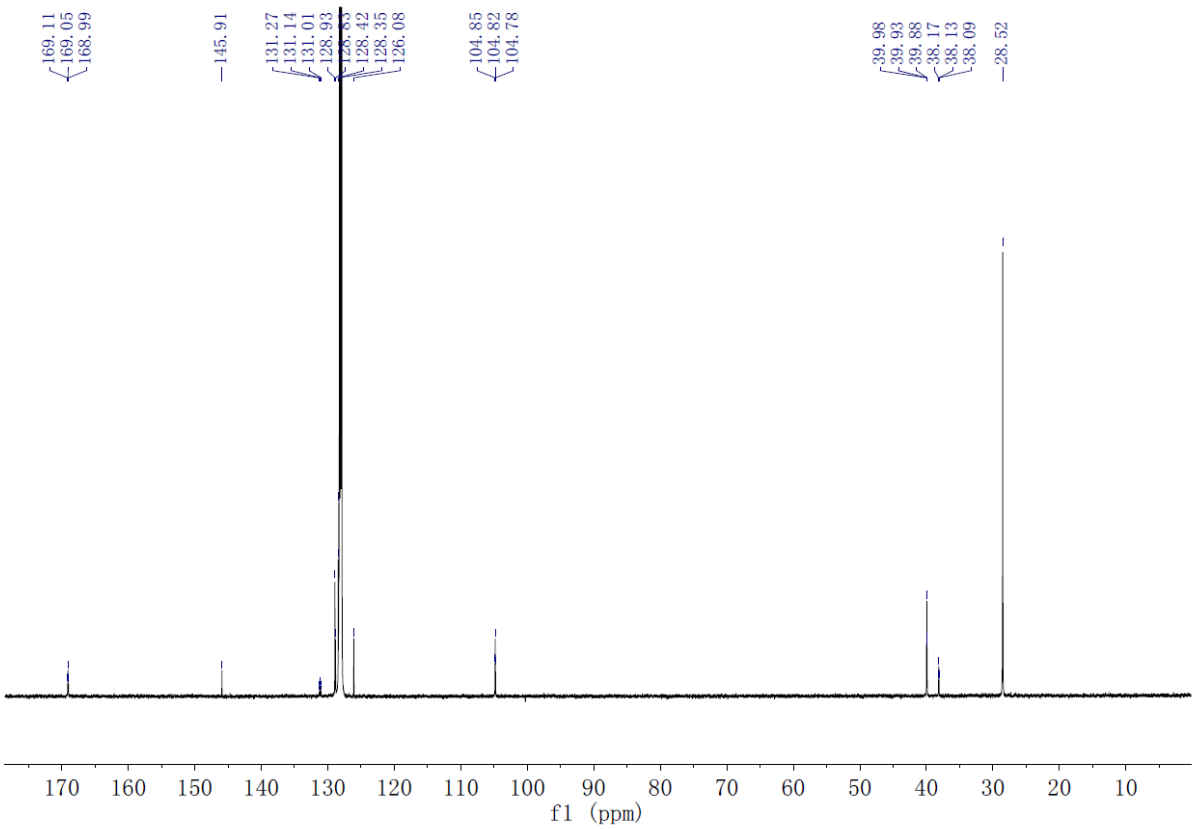

Figure S14 ^{13}C{^{1}H} NMR spectrum of **2** (benzene-d_6)

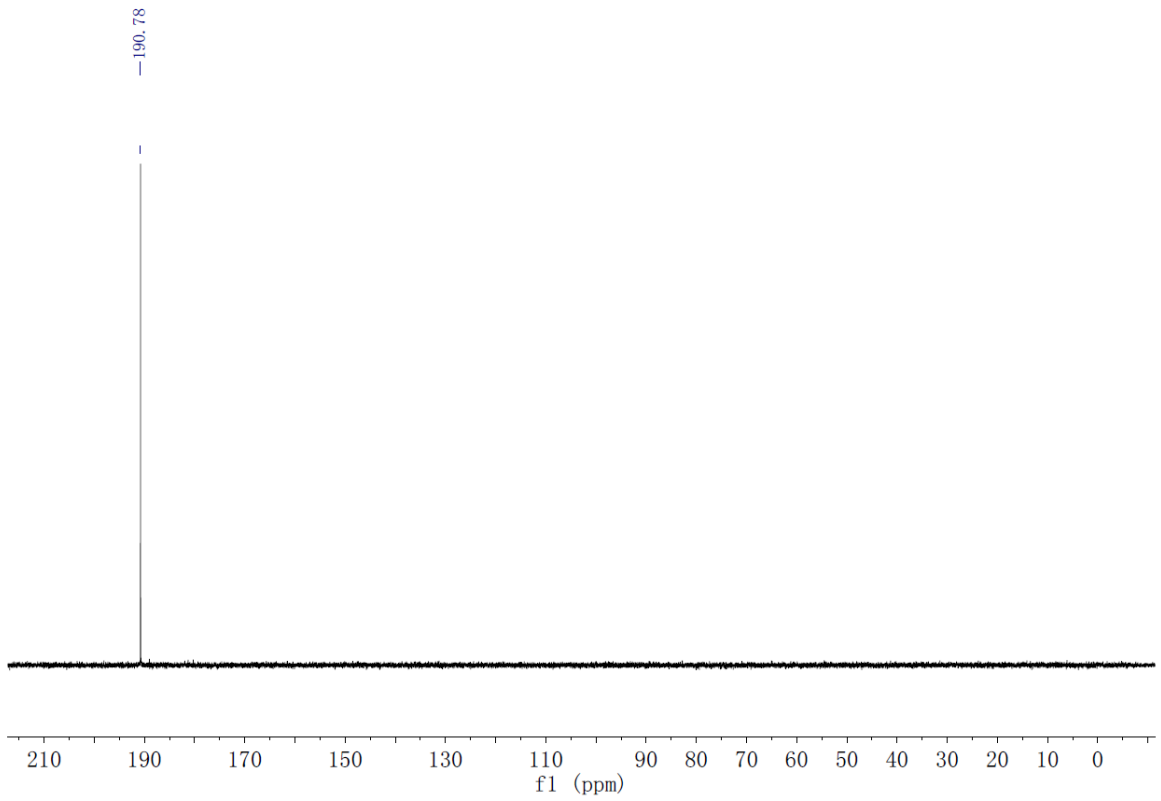

Figure S15 $^{31}P\{^{1}H\}$ NMR spectrum of **2** (benzene-d_6)

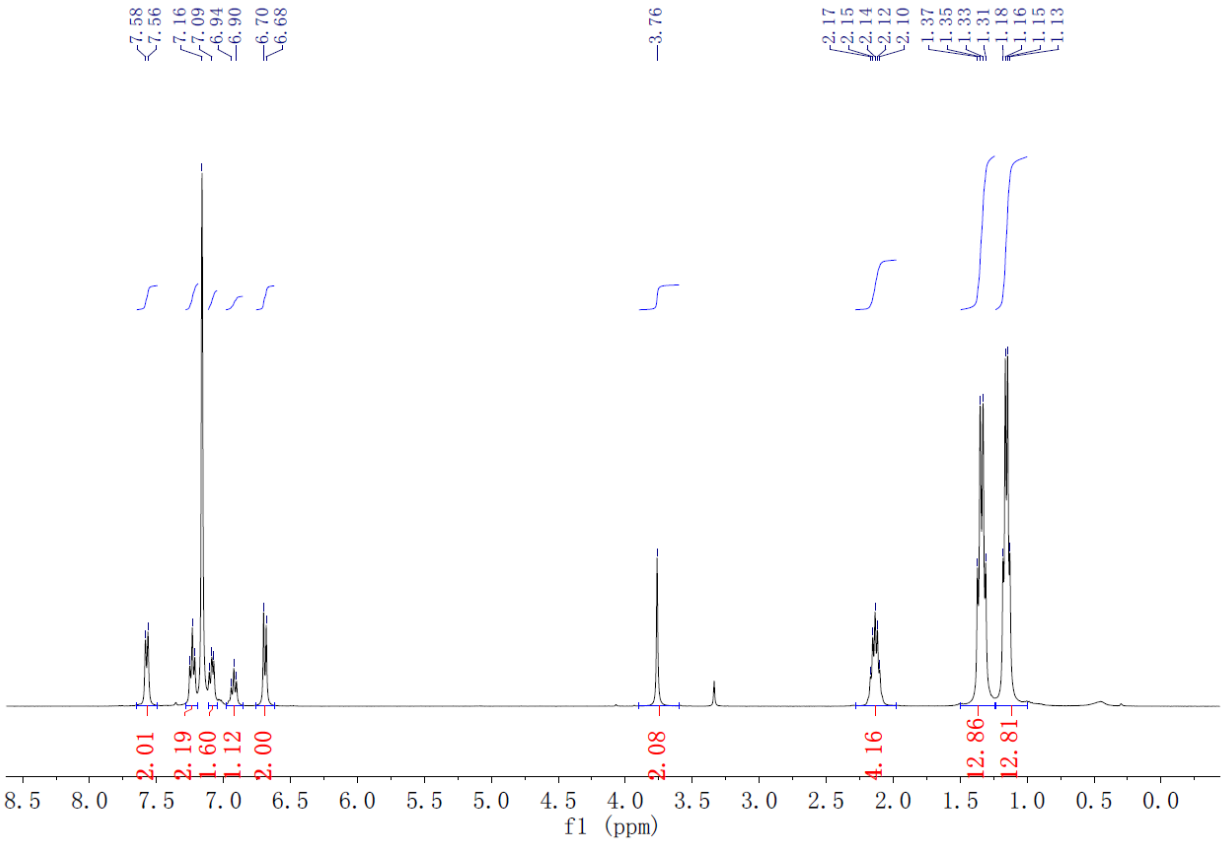

Figure S16 ^{1}H NMR spectrum of **4** (benzene-d_6)

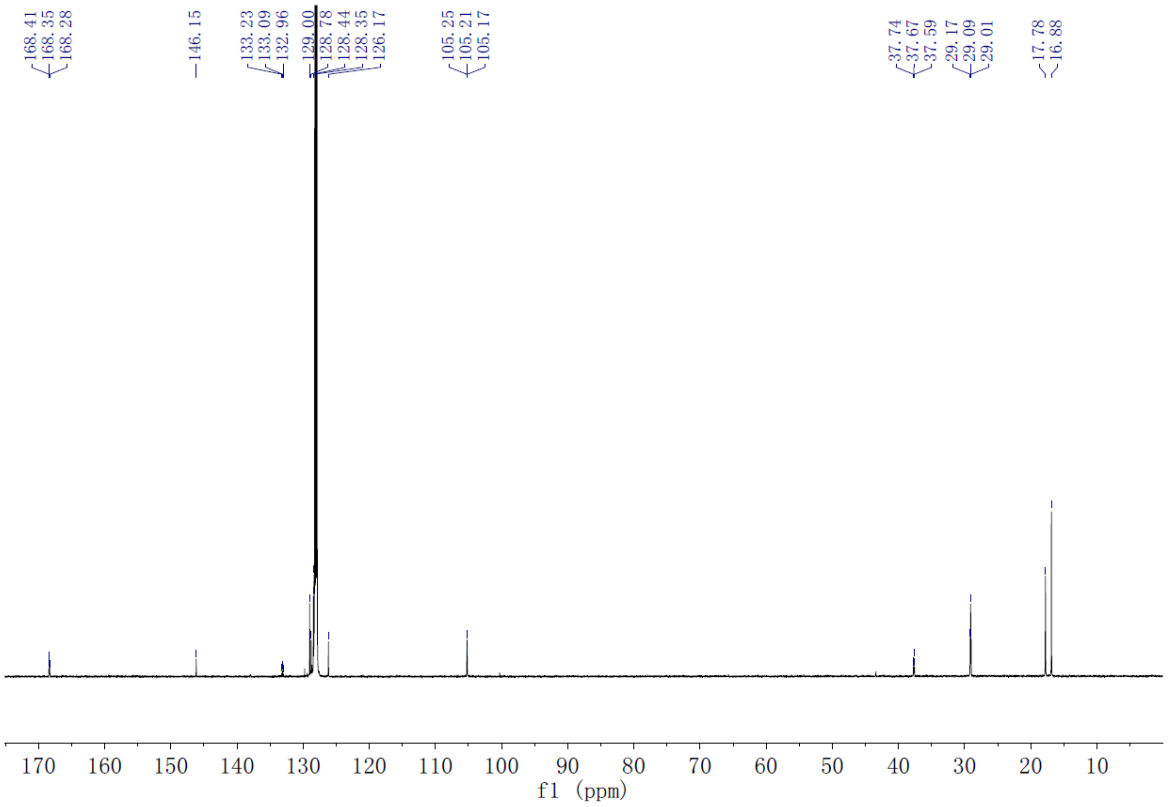

Figure S17 $^{13}C\{^{1}H\}$ NMR spectrum of **4** (benzene-d_6)

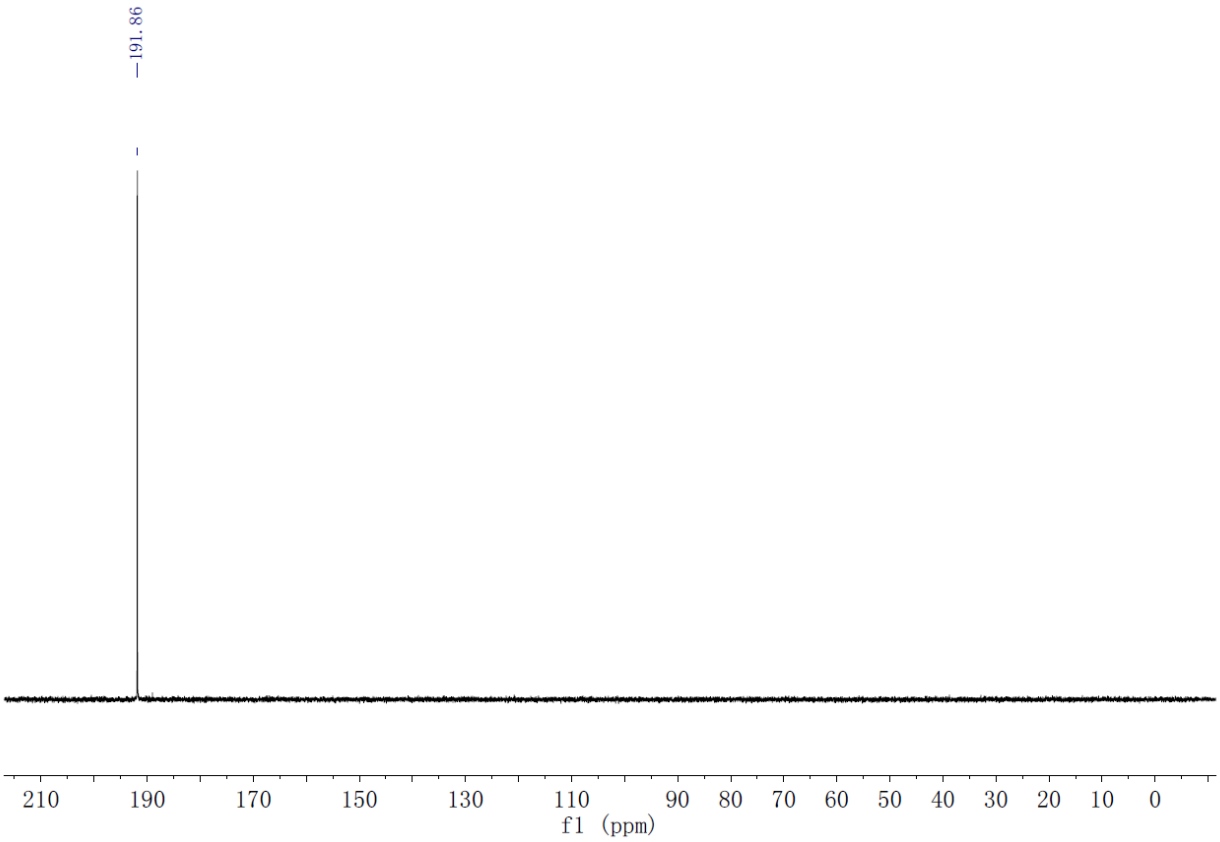

Figure S18 $^{31}P\{^{1}H\}$ NMR spectrum of **4** (benzene-d_6)

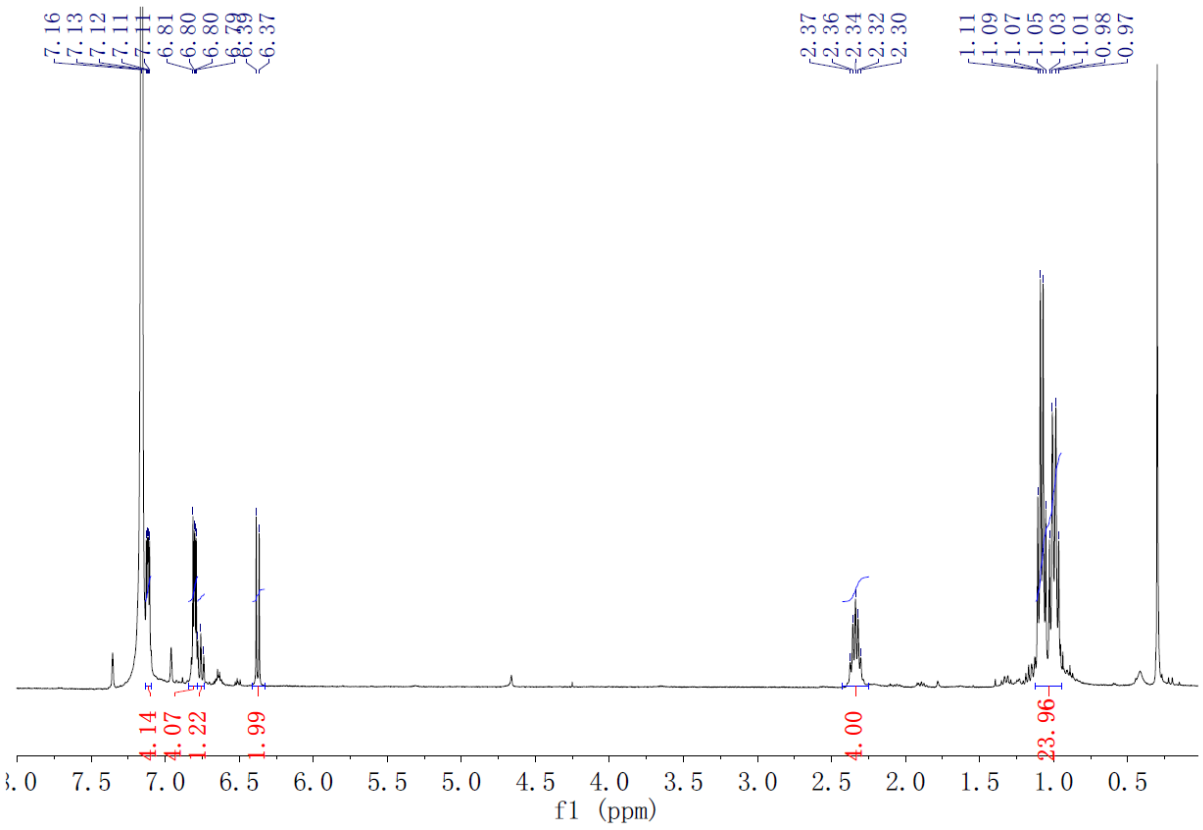

Figure S19 ^{1}H NMR spectrum of **6** (benzene-d_6)

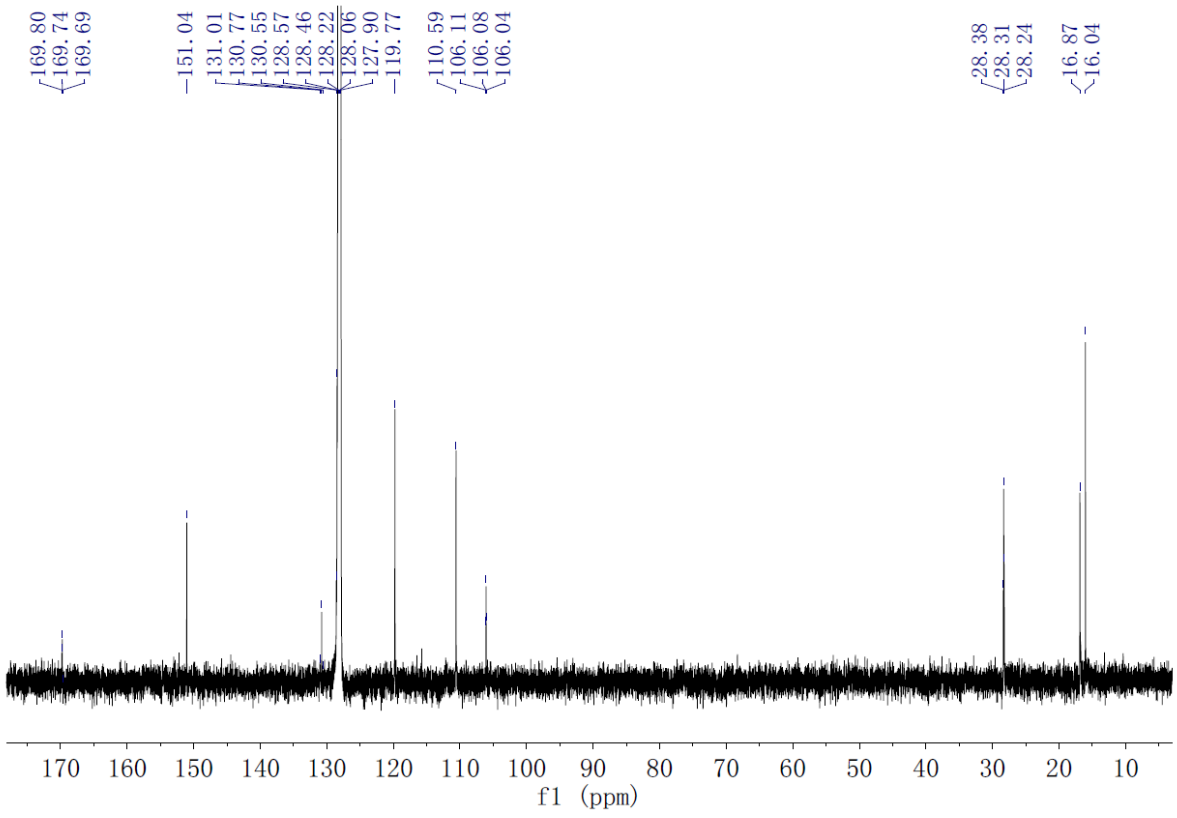

Figure S20 ^{13}C{^{1}H} NMR spectrum of **6** (benzene-d_6)

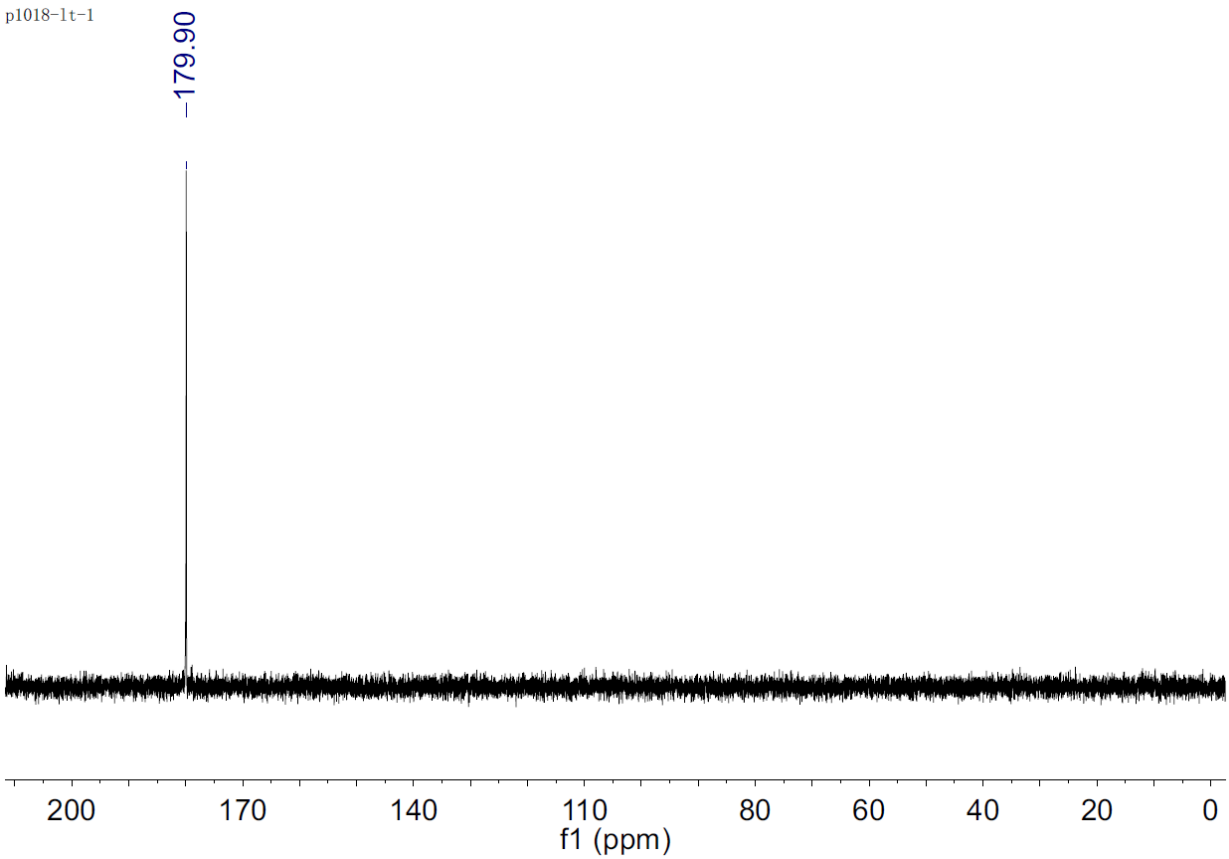

Figure S21 $^{31}P\{^{1}H\}$ NMR spectrum of **6** (benzene-d_6)

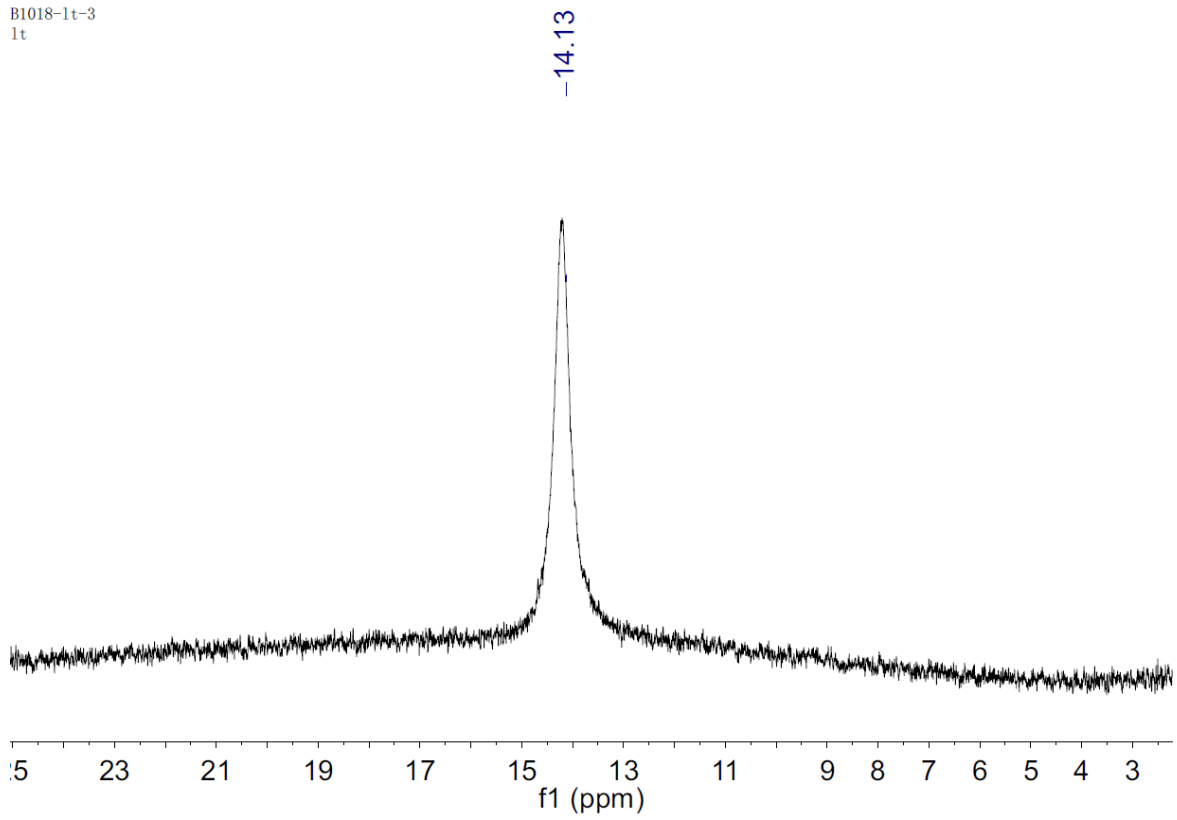

Figure S22 ^{11}B NMR spectrum of **6** (benzene-d_6)

Mass Spectrum SmartFormula Report

Analysis Info

Analysis Name	D:\Data\zhang\20160309\6.d	Acquisition Date	3/9/2016 10:42:49 AM
Method	tune_low_pos120731.m	Operator	zym
Sample Name	hy-7new	Instrument / Ser#	micrOTOF 10376
Comment			

Acquisition Parameter

Source Type	ESI	Ion Polarity	Positive	Set Nebulizer	0.3 Bar
Focus	Active			Set Dry Heater	180 °C
Scan Begin	50 m/z	Set Capillary	4500 V	Set Dry Gas	4.0 l/min
Scan End	1500 m/z	Set End Plate Offset	-500 V	Set Divert Valve	Waste

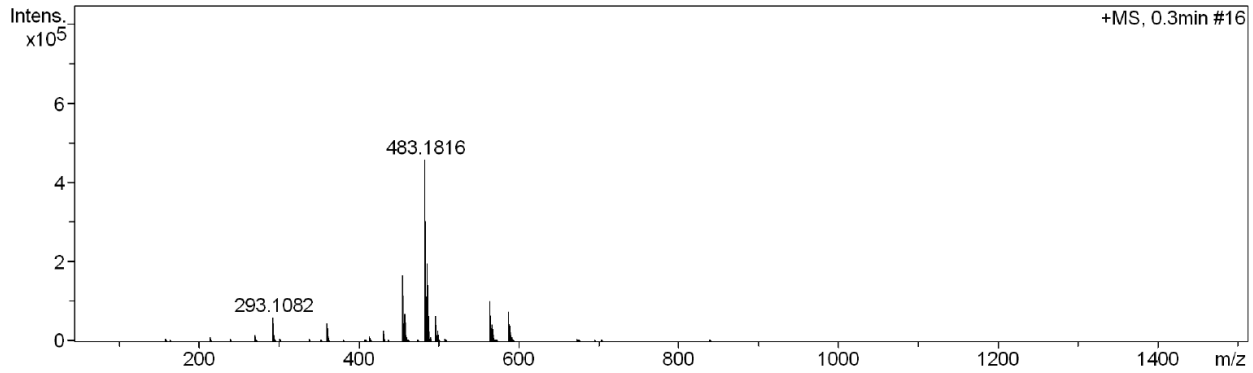

Meas. m/z	#	Formula	Score	m/z	err [ppm]	Mean err [ppm]	mSigma	rdb	e⁻ Conf	N-Rule
564.1876	1	C 28 H 37 N 5 Ni P S	100.00	564.1855	-3.8	-2.4	23.7	13.5	even	ok
	2	C 28 H 30 N 5 O 6 S	0.03	564.1911	6.2	7.9	170.9	16.5	even	ok
	3	C 28 H 18 N 15	0.02	564.1864	-2.2	5.2	197.7	27.5	even	ok
587.1760	1	C 28 H 44 Na Ni O 2 P 2 S	100.00	587.1783	3.8	3.6	25.3	7.5	even	ok

Figure S23 HRMS (ESI) spectrum of **1c**

Mass Spectrum SmartFormula Report

Analysis Info

Analysis Name	D:\Data\zhang\20160309\7.d	Acquisition Date	3/9/2016 10:48:05 AM
Method	tune_low_pos120731.m	Operator	zym
Sample Name	hy-7new	Instrument / Ser#	micrOTOF 10376
Comment			

Acquisition Parameter

Source Type	ESI	Ion Polarity	Positive	Set Nebulizer	0.3 Bar
Focus	Active			Set Dry Heater	180 °C
Scan Begin	50 m/z	Set Capillary	4500 V	Set Dry Gas	4.0 l/min
Scan End	1500 m/z	Set End Plate Offset	-500 V	Set Divert Valve	Waste

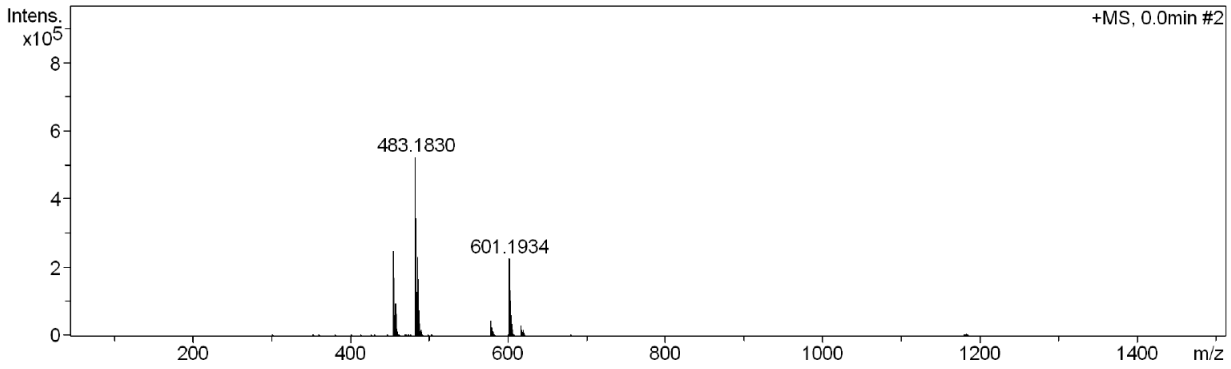

Meas. m/z	#	Formula	Score	m/z	err [ppm]	Mean err [ppm]	mSigma	rdb	e⁻ Conf	N-Rule
601.1934	1	C 29 H 46 Na Ni O 2 P 2 S	100.00	601.1939	0.9	1.3	9.6	7.5	even	ok

Figure S24 HRMS (ESI) spectrum of **2**

Mass Spectrum SmartFormula Report

Analysis Info

Analysis Name	D:\Data\zhang\20160311\3 .d	Acquisition Date	3/11/2016 9:10:20 AM
Method	tune_low_pos120731.m	Operator	zym
Sample Name	hy-7new	Instrument / Ser#	micrOTOF 10376
Comment			

Acquisition Parameter

Source Type	ESI	Ion Polarity	Positive	Set Nebulizer	0.3 Bar
Focus	Active			Set Dry Heater	180 °C
Scan Begin	50 m/z	Set Capillary	4500 V	Set Dry Gas	4.0 l/min
Scan End	1000 m/z	Set End Plate Offset	-500 V	Set Divert Valve	Waste

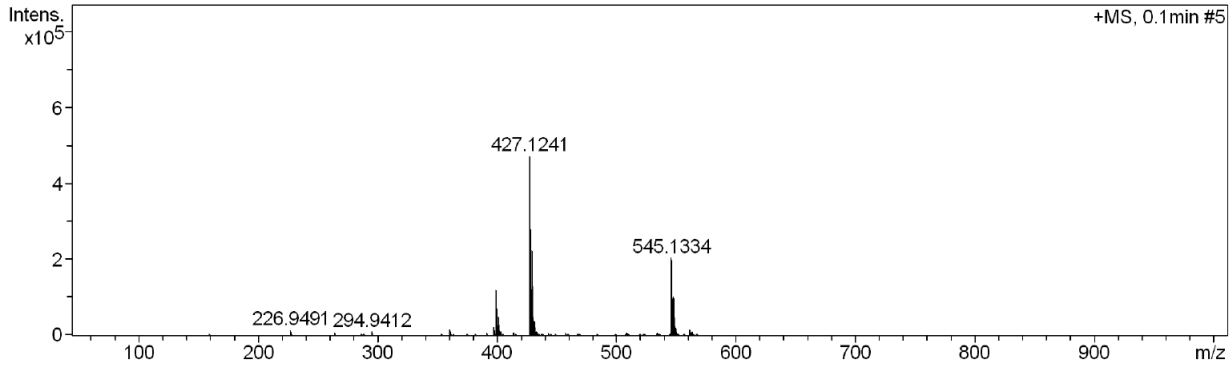

Meas. m/z	#	Formula	Score	m/z	err [ppm]	Mean err [ppm]	mSigma	rdb	e⁻ Conf	N-Rule
545.1334	1	C 25 H 38 Na Ni O 2 P 2 S	100.00	545.1313	-3.8	-5.0	19.8	7.5	even	ok

Figure S25 HRMS (ESI) spectrum of **4**

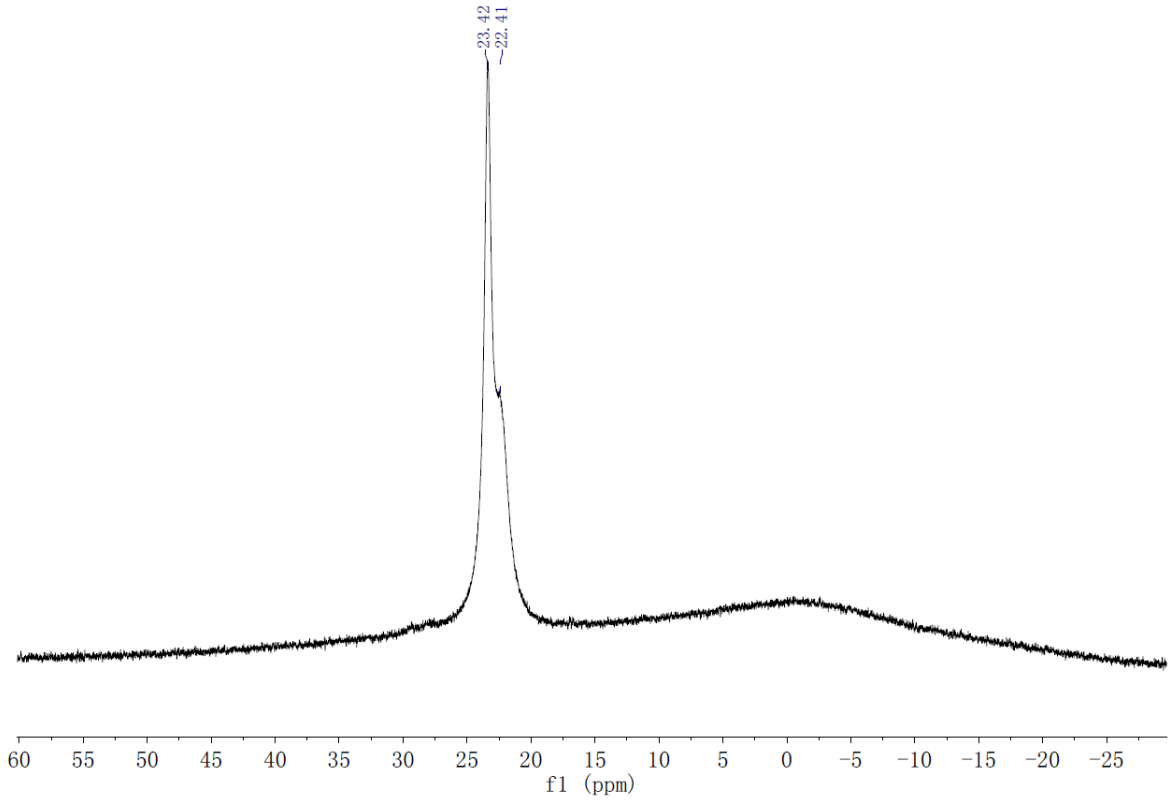

Figure S26 ^{11}B NMR spectrum of the clear solution after catalytic hydroboration of CO_2 with HBcat. Conditions: 0.011 mmol **1c**, 5.5 mmol HBcat, 4 mL C_6D_6, 1 atm CO_2, 0.022 mmol C_6Me_6, RT.

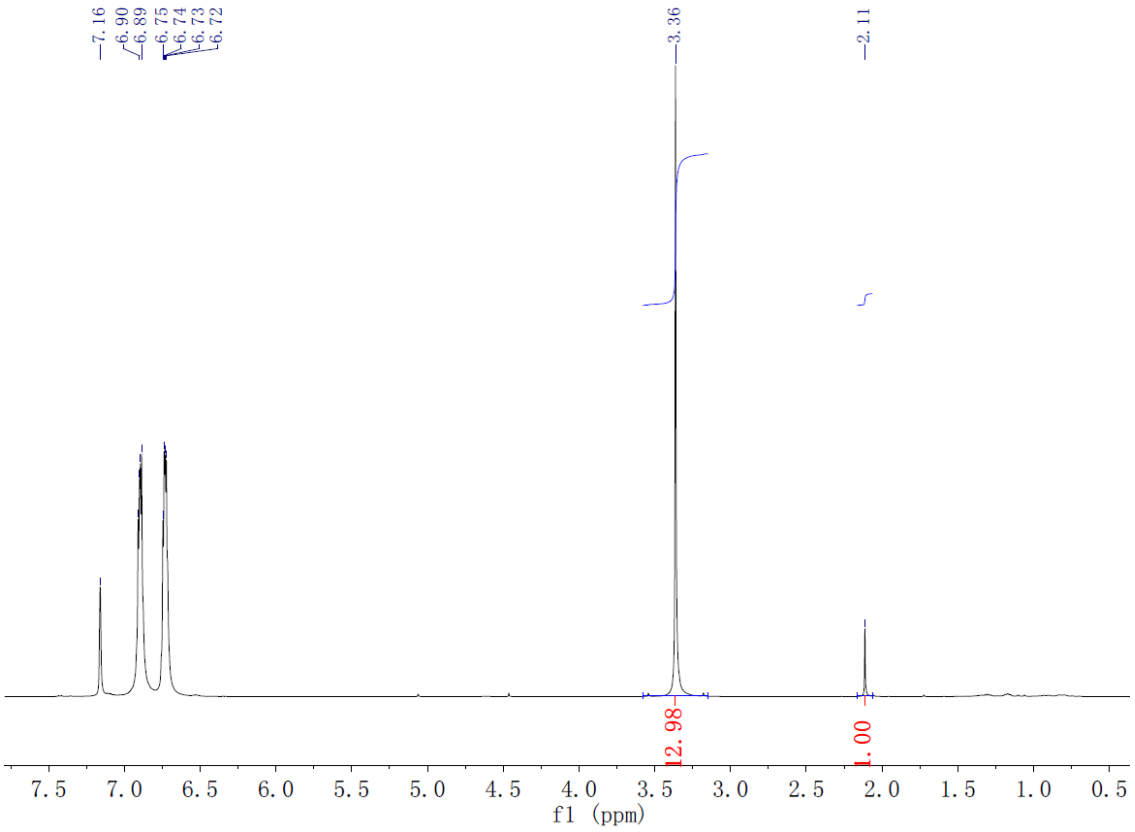

Figure S27 ^{1}H NMR spectrum of the clear solution after catalytic hydroboration of CO_2 with HBcat. Conditions: 0.011 mmol **1c**, 5.5 mmol HBcat, 4 mL C_6D_6, 1 atm CO_2, 0.022 mmol C_6Me_6, RT.

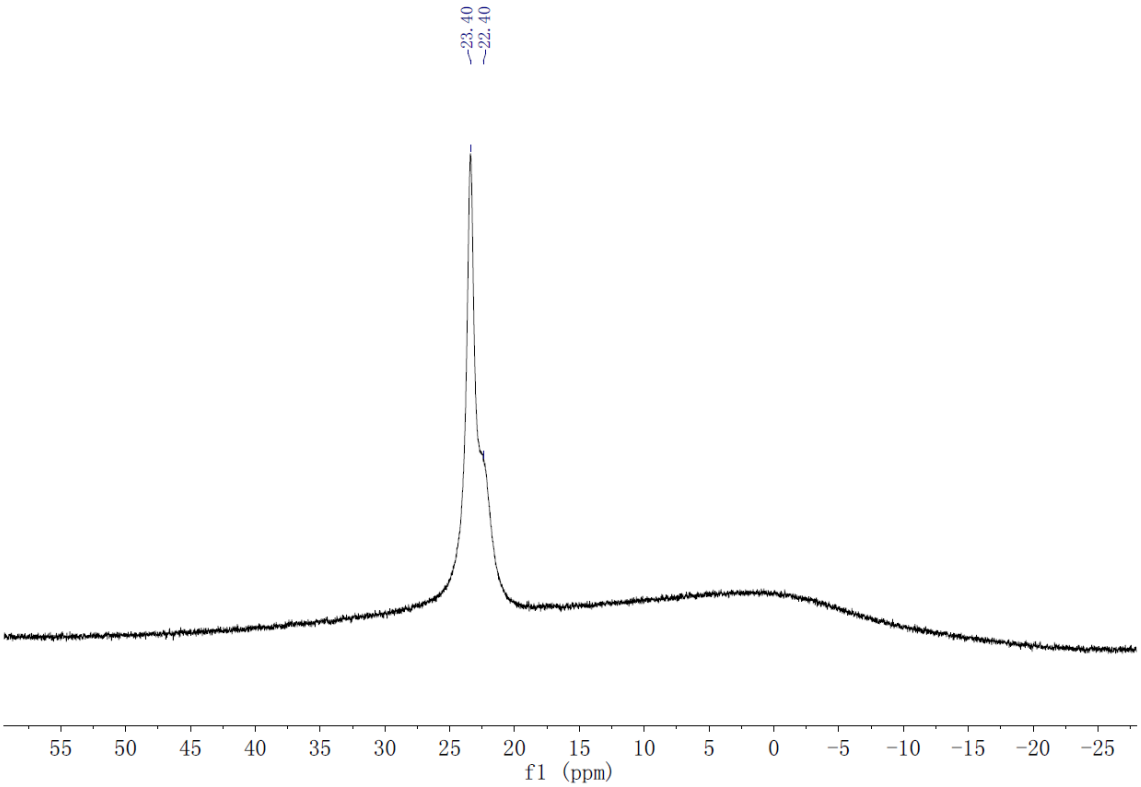

Figure S28 ^{11}B NMR spectrum of the clear solution after catalytic hydroboration of CO_2 with HBcat. Conditions: 0.011 mmol **2**, 5.5 mmol HBcat, 4 mL C_6D_6, 1 atm CO_2, 0.022 mmol C_6Me_6, RT.

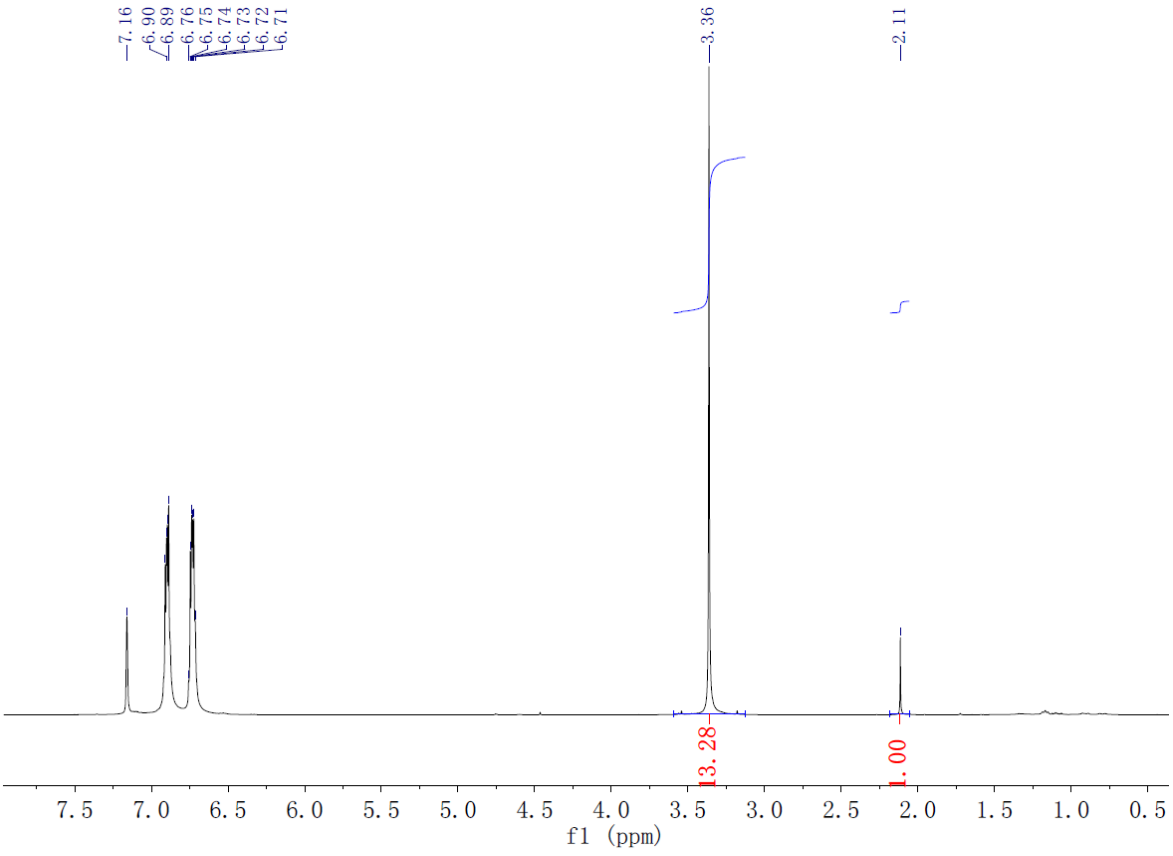

Figure S29 ^{1}H NMR spectrum of the clear solution after catalytic hydroboration of CO_2 with HBcat. Conditions: 0.011 mmol **2**, 5.5 mmol HBcat, 4 mL C_6D_6, 1 atm CO_2, 0.022 mmol C_6Me_6, RT.

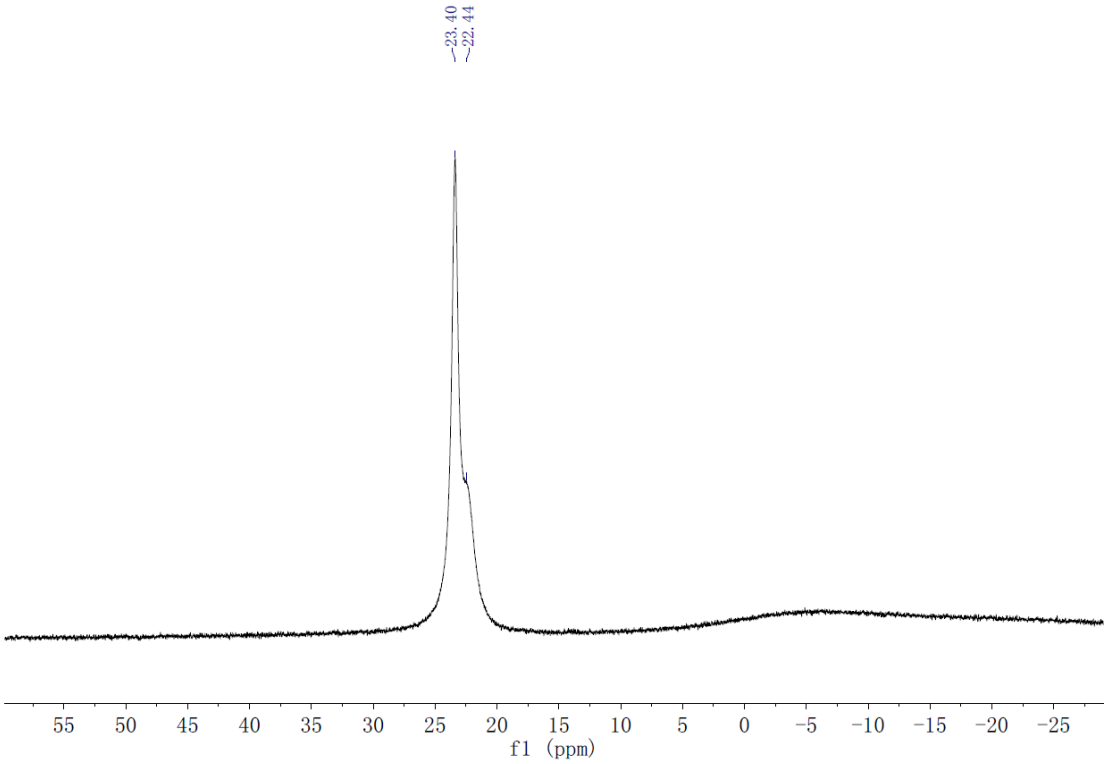

Figure S30 ^{11}B NMR spectrum of the clear solution after catalytic hydroboration of CO_2 with HBcat. Conditions: 0.011 mmol **3c**, 5.5 mmol HBcat, 4 mL C_6D_6, 1 atm CO_2, 0.022 mmol C_6Me_6, RT.

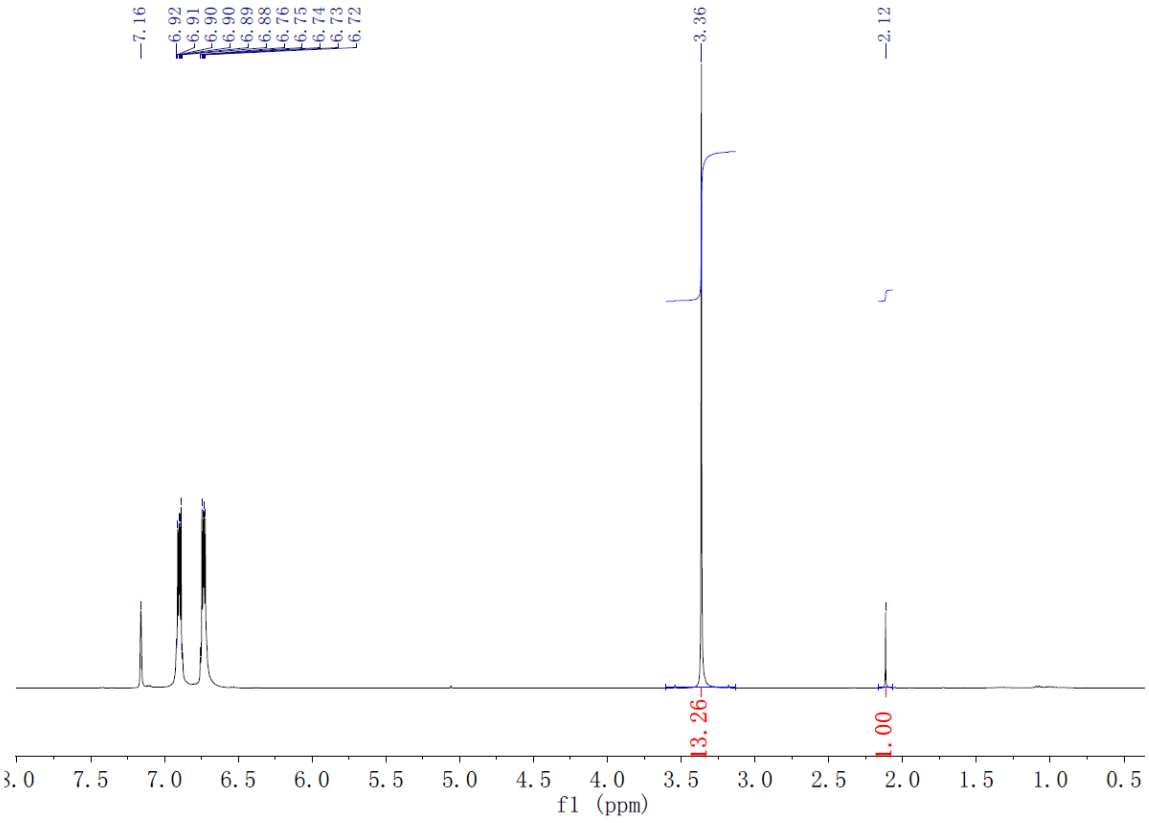

Figure S31 ^{1}H NMR spectrum of the clear solution after catalytic hydroboration of CO_2 with HBcat. Conditions: 0.011 mmol **3c**, 5.5 mmol HBcat, 4 mL C_6D_6, 1 atm CO_2, 0.022 mmol C_6Me_6, RT.

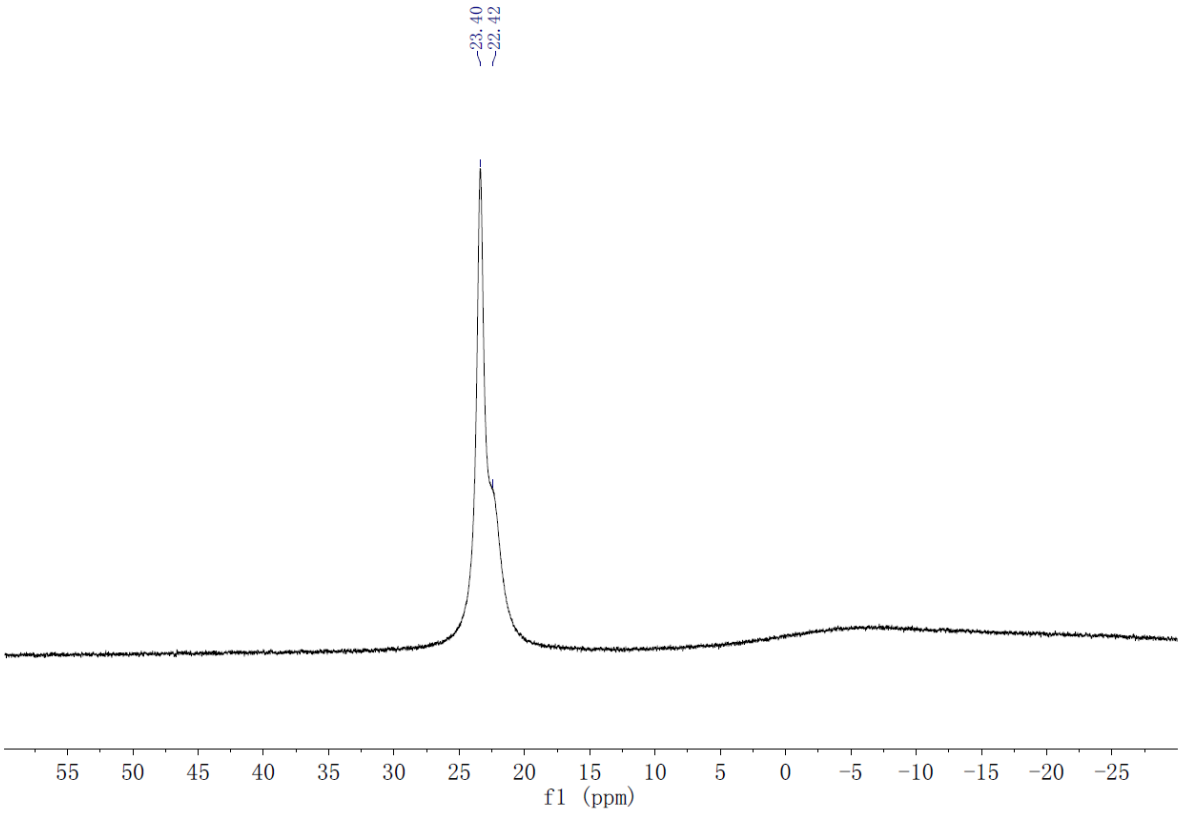

Figure S32 ^{11}B NMR spectrum of the clear solution after catalytic hydroboration of CO_2 with HBcat. Conditions: 0.011 mmol **4**, 5.5 mmol HBcat, 4 mL C_6D_6, 1 atm CO_2, 0.022 mmol C_6Me_6, RT.

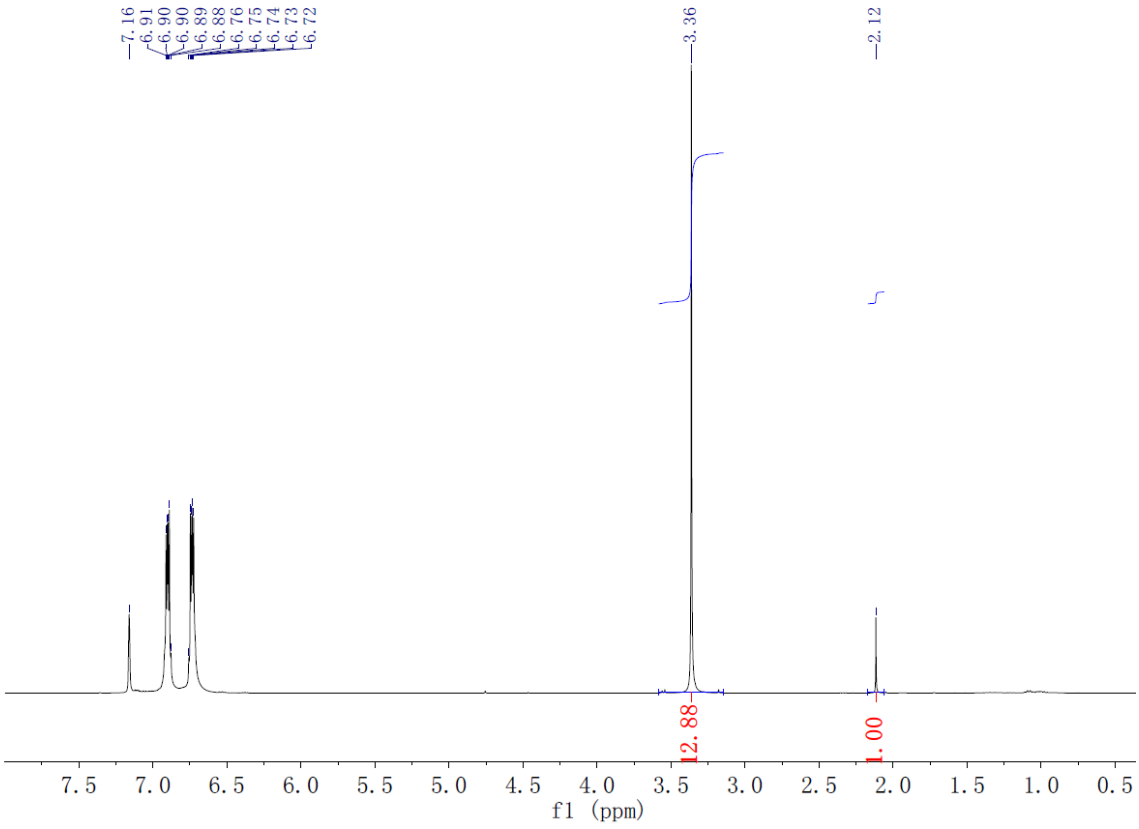

Figure S33 ^{1}H NMR spectrum of the clear solution after catalytic hydroboration of CO_2 with HBcat. Conditions: 0.011 mmol **4**, 5.5 mmol HBcat, 4 mL C_6D_6, 1 atm CO_2, 0.022 mmol C_6Me_6, RT.

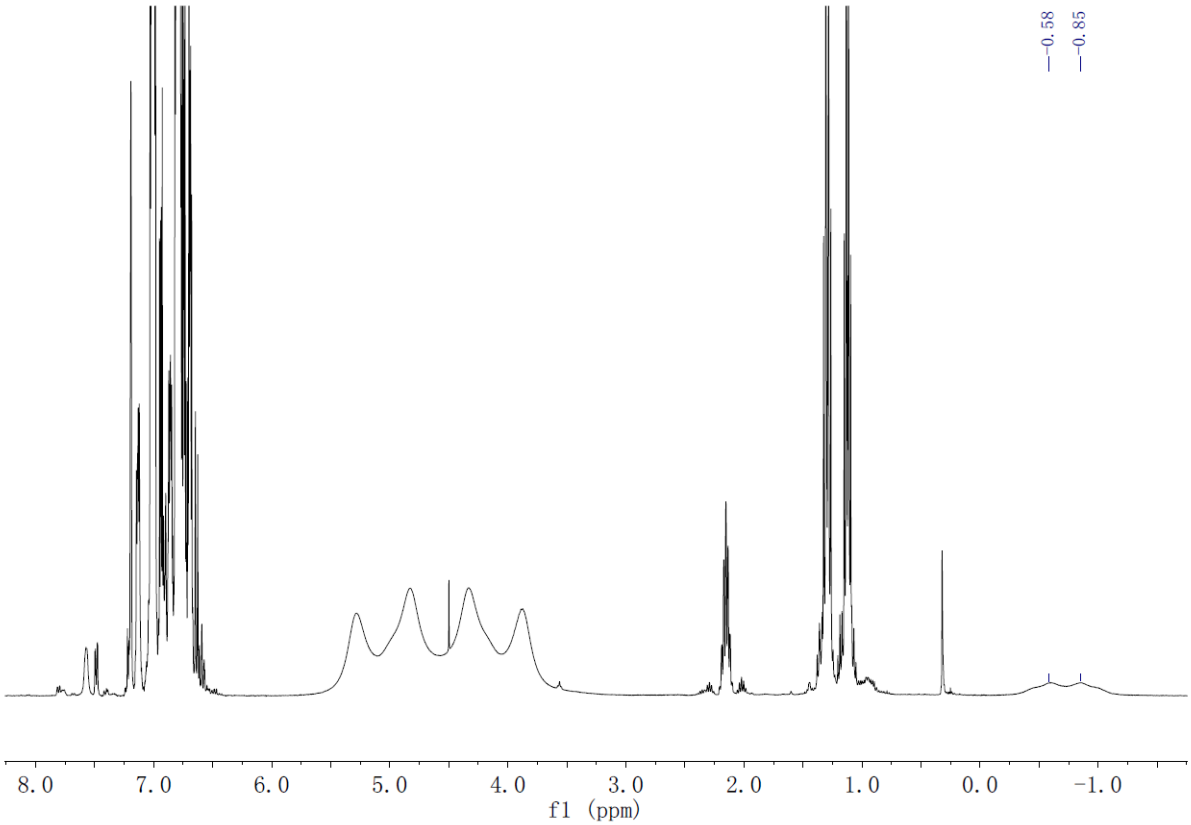

Figure S34 ^{1}H NMR spectrum of the interaction of **3c** with 30 equiv of HBcat in C_6D_6 at room temperature (spectrum was recorded after overnight).

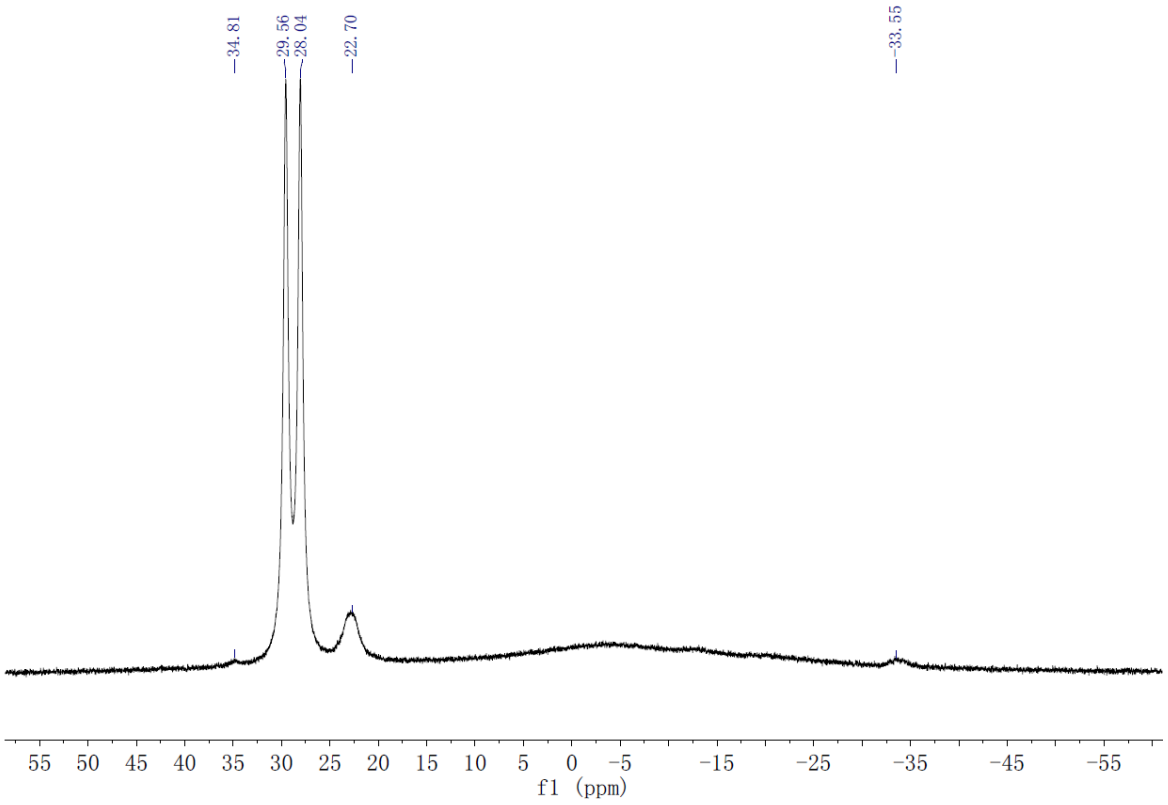

Figure S35 ^{11}B NMR spectrum of the interaction of **3c** with 30 equiv of HBcat in C_6D_6 at room temperature (spectrum was recorded after overnight).

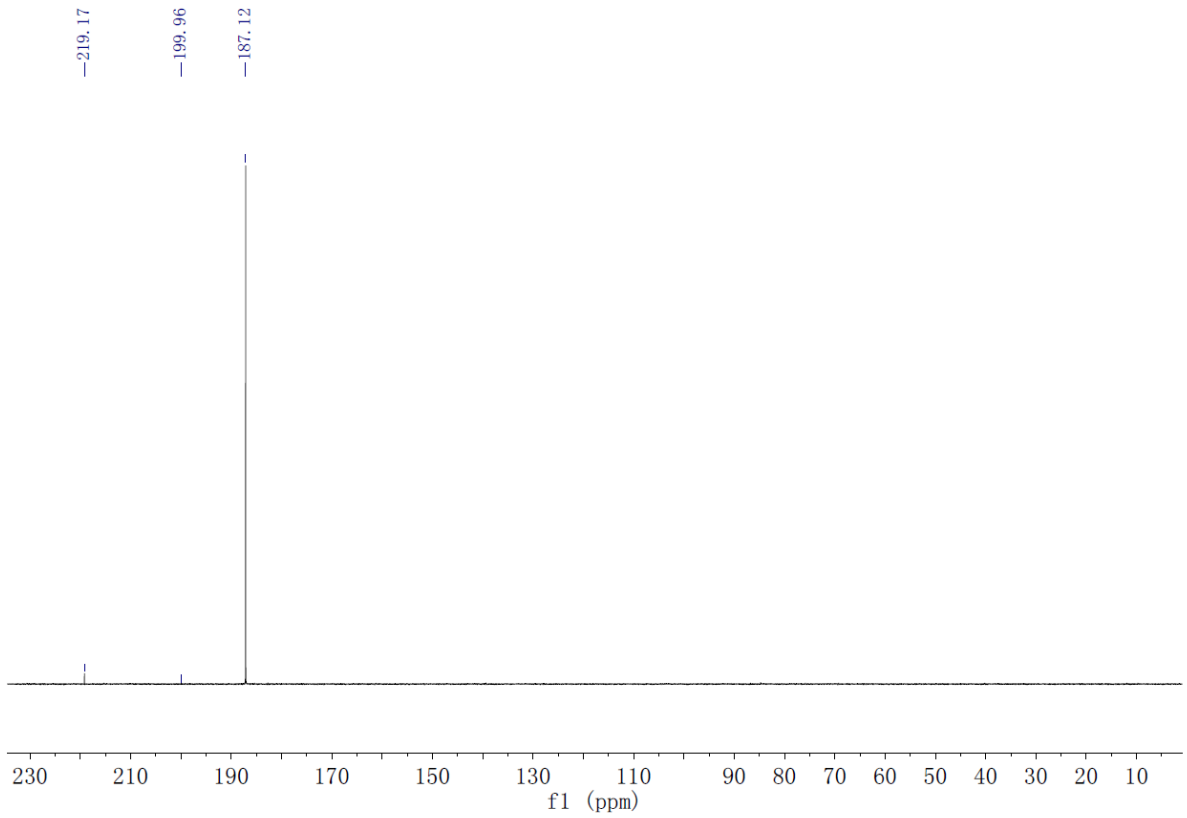

Figure S36 $^{31}P\{^{1}H\}$ NMR spectrum of the interaction of **1c** with 5 equiv of HBcat in C_6D_6 at room temperature (spectrum was recorded 30 min after mixing **1c** and HBcat).

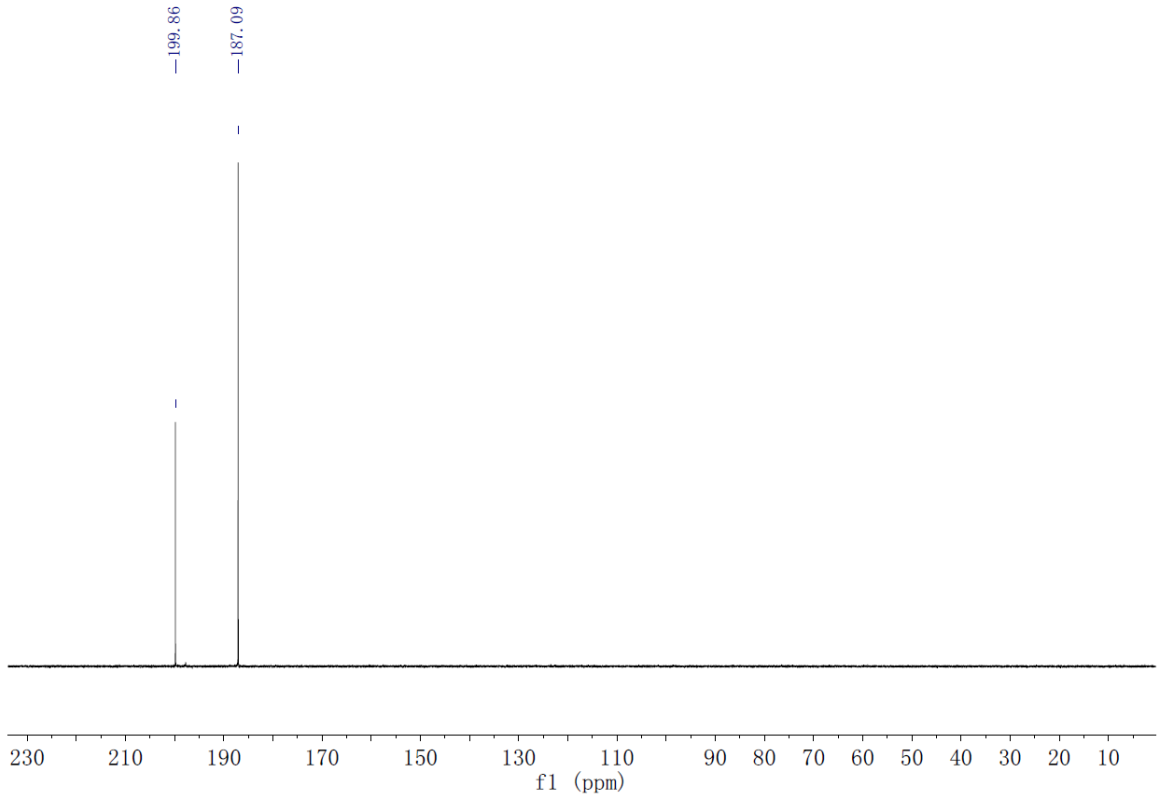

Figure S37 $^{31}P\{^{1}H\}$ NMR spectrum of the interaction of **1c** with 30 equiv of HBcat in C_6D_6 at room temperature (spectrum was recorded 30 min after mixing **1c** and HBcat).

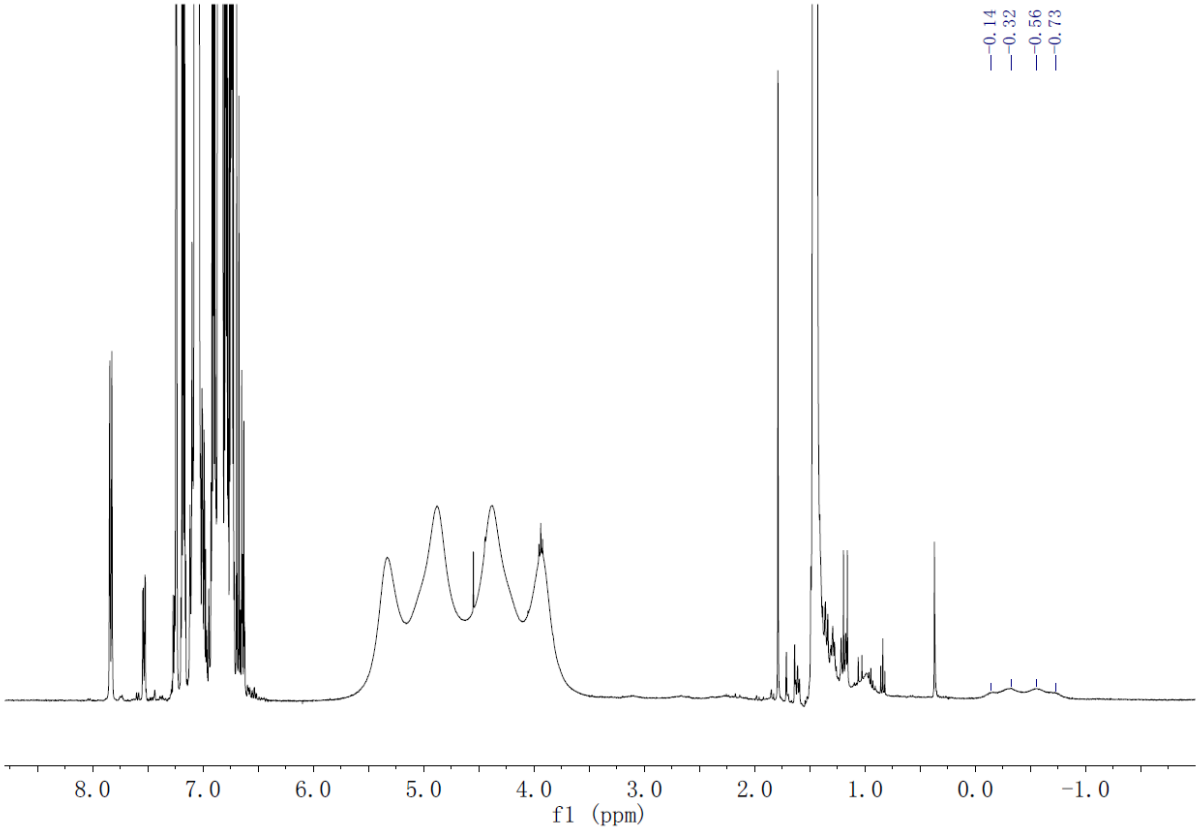

Figure S38 ^{1}H NMR spectrum of the interaction of **1c** with 30 equiv of HBcat in C_6D_6 at room temperature (spectrum was recorded 30 min after mixing **1c** and HBcat).

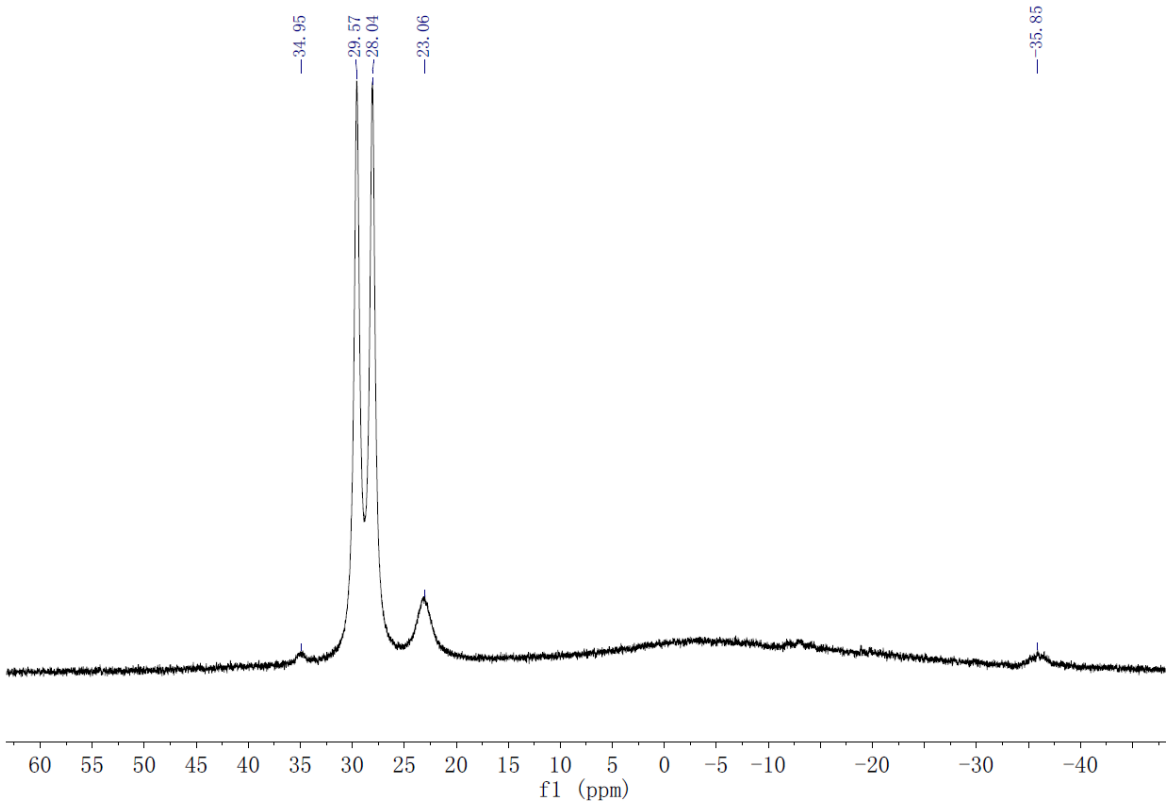

Figure S39 ^{11}B NMR spectrum of the interaction of **1c** with 30 equiv of HBcat in C_6D_6 at room temperature (spectrum was recorded 30 min after mixing **1c** and HBcat).

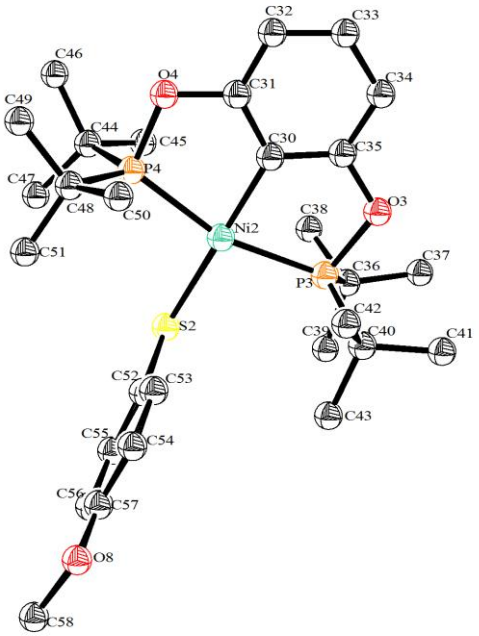

Figure S40 Thermal ellipsoid plots of complex **1a** at the 50% probability level (Three independent molecules were found in the crystalline lattice; only one is shown here).

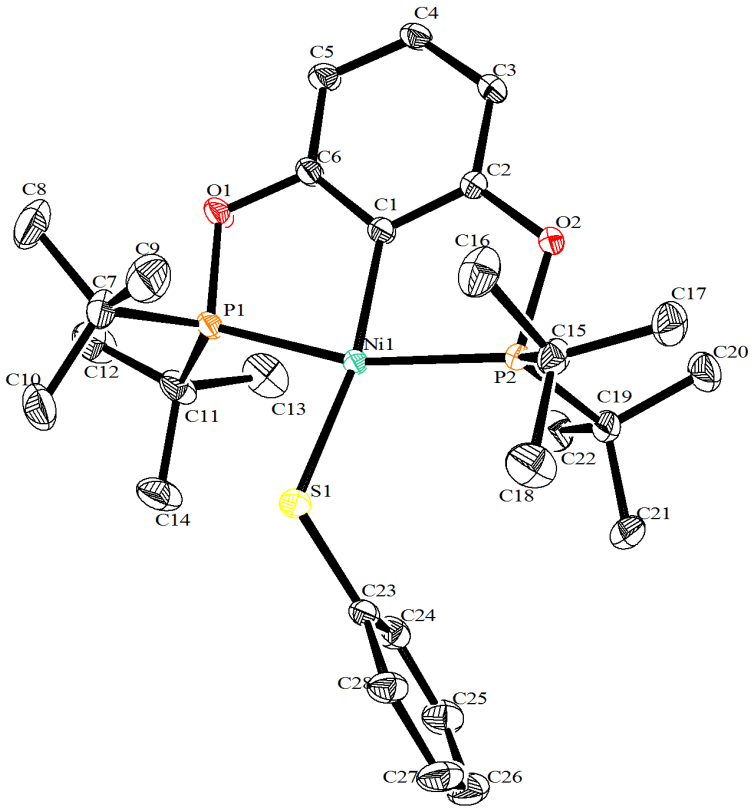

Figure S41 Thermal ellipsoid plots of **1c** at the 50 % probability level. Hydrogen atoms are omitted for clarity.

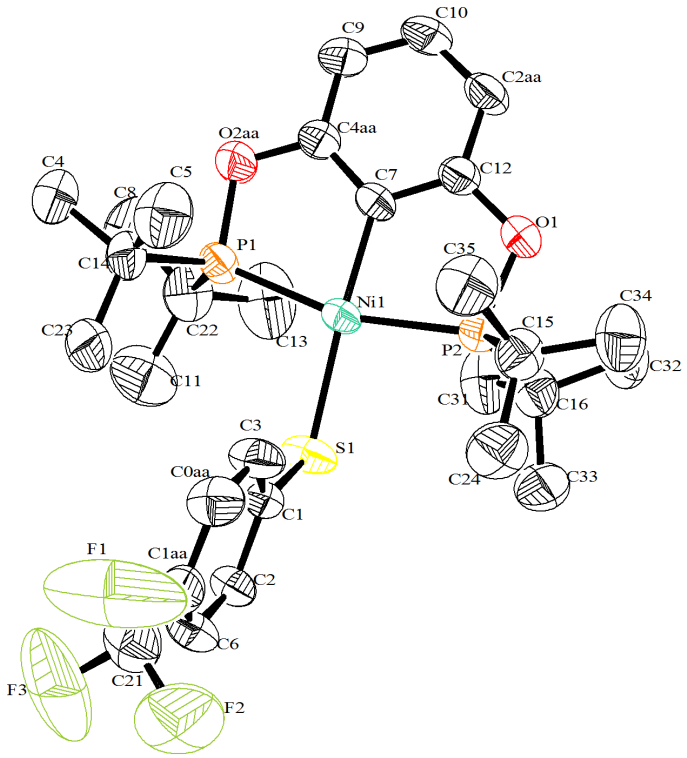

Figure S42 Thermal ellipsoid plots of **1d** at the 50 % probability level. Hydrogen atoms are omitted for clarity.

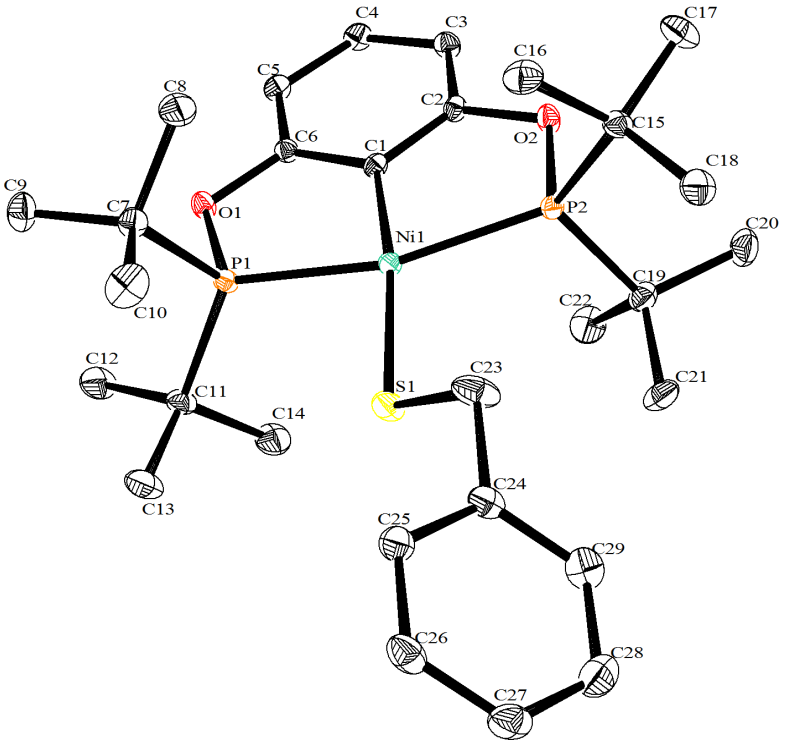

Figure S43 Thermal ellipsoid plots of **2** at the 50 % probability level. Hydrogen atoms are omitted for clarity. (Two independent molecules were found in the crystalline lattice; only one is shown here).

XRD analysis confirmation of the formation of [2,6-(^{t}Bu$_2$PO)$_2$C$_6$H$_3$]Ni(η^2-BH$_4$)

A crystal developed in the NMR tube for the interaction of **1c** with 30 equiv of HBcat in C_6D_6 after a few days. In order to identify this crystal, X-ray diffraction analysis was carried out. The experimental technique was similar to that used for the structure determination of **2**. The analysis results confirmed that the crystal is [2,6-(^{t}Bu$_2$PO)$_2$C$_6$H$_3$]Ni(η^2-BH$_4$). The crystal structure of this complex has already been reported before. For comparison the analysis results of the present study are presented in this supporting information. Crystal data collection and refinement parameters are summarized in Table S1; the structure is shown in Figure S44; atomic coordinates and equivalent isotropic atomic displacement parameters are listed in Table S2; bond lengths and angles are provided in Table S3; anisotropic atomic displacement parameters are presented in Table S4; hydrogen atomic coordinates and isotropic atomic displacement parameters are given in Table S5.

Table S1 Summary of crystal data and structure refinement for [2,6-(^{t}Bu$_2$PO)$_2$C$_6$H$_3$]Ni(η^2-BH$_4$)

Empirical formula	$C_{22}H_{43}BNiO_2P_2$
Formula weight	471.02
Temp, K	103(2)
Crystal system	Triclinic
Space group	P -1
a, Å	8.2685(8)
b, Å	12.1130(12)
c, Å	13.3986(13)
α (°)	100.327(3)
β (°)	95.741(3)
γ (°)	104.978(3)
Volume, Å^3	1260.1(2)
Z	2
d_{calc}, g cm^{-3}	1.241
λ, Å	0.71073
μ, mm^{-1}	0.911
No. of data collected	39389
No. of unique data	8109
R_{int}	0.1065
Goodness-of-fit on F^2	1.020
R_1, wR_2 ($I > 2\sigma(I)$)	0.0461, 0.1040
R_1, wR_2 (all data)	0.0678, 0.1161

Table S2 Atomic coordinates and equivalent isotropic atomic displacement parameters ($Å^2$) of

$[2,6\text{-}(^tBu_2PO)_2C_6H_3]Ni((\eta^2\text{-}BH_4)$

U(eq) is defined as one third of the trace of the orthogonalized U_{ij} tensor.

	x/a	y/b	z/c	U(eq)
Ni1	0.46761(3)	0.26015(2)	0.23103(2)	0.01050(7)
B1	0.3190(3)	0.2650(2)	0.08570(19)	0.0202(5)
C1	0.5974(2)	0.25645(17)	0.35487(14)	0.0107(3)
C2	0.7397(2)	0.34793(16)	0.40478(13)	0.0102(3)
C3	0.8380(3)	0.34719(18)	0.49460(14)	0.0135(4)
C4	0.7947(3)	0.24951(17)	0.53787(14)	0.0137(4)
C5	0.6540(3)	0.15563(18)	0.49319(14)	0.0143(4)
C6	0.5599(2)	0.16161(17)	0.40357(14)	0.0117(4)
C7	0.3186(3)	0.95576(18)	0.16259(15)	0.0146(4)
C8	0.5065(3)	0.9652(2)	0.15886(19)	0.0255(5)
C9	0.2376(3)	0.84322(19)	0.19719(17)	0.0238(5)
C10	0.2315(3)	0.9504(2)	0.05462(16)	0.0250(5)
C11	0.1089(3)	0.08770(19)	0.29497(15)	0.0167(4)
C12	0.0491(3)	0.9950(2)	0.35849(19)	0.0282(5)
C13	0.9737(3)	0.0705(2)	0.20250(18)	0.0237(5)
C14	0.1371(3)	0.2088(2)	0.36452(18)	0.0268(5)
C15	0.8184(3)	0.44088(18)	0.16370(14)	0.0137(4)
C16	0.8808(3)	0.3324(2)	0.16547(19)	0.0265(5)
C17	0.9712(3)	0.5484(2)	0.19947(19)	0.0334(6)
C18	0.7403(3)	0.4343(3)	0.05341(17)	0.0304(6)
C19	0.5858(3)	0.56472(18)	0.28424(15)	0.0160(4)
C20	0.7303(3)	0.6742(2)	0.3360(2)	0.0351(6)
C21	0.4923(4)	0.5884(2)	0.18954(19)	0.0327(6)
C22	0.4622(5)	0.5381(3)	0.3599(2)	0.0480(9)
O1	0.41874(18)	0.06904(12)	0.35911(10)	0.0136(3)
O2	0.78273(18)	0.44554(11)	0.36135(10)	0.0122(3)
P1	0.31844(6)	0.09046(4)	0.25449(4)	0.01070(10)
P2	0.65802(6)	0.43080(4)	0.25247(4)	0.01023(10)

Table S3 Bond lengths (Å) and angles (°) of [2,6-(^{t}Bu$_2$PO)$_2$C$_6$H$_3$]Ni(η^2-BH$_4$)

Ni1-C1	1.8978(18)	Ni1-P1	2.2009(6)
Ni1-P2	2.2020(6)	Ni1-B1	2.215(2)
C1-C2	1.401(3)	C1-C6	1.402(3)
C2-C3	1.386(2)	C2-O2	1.391(2)
C3-C4	1.390(3)	C4-C5	1.392(3)
C5-C6	1.388(2)	C6-O1	1.385(2)
C7-C9	1.529(3)	C7-C10	1.533(3)
C7-C8	1.535(3)	C7-P1	1.860(2)
C11-C13	1.529(3)	C11-C14	1.538(3)
C11-C12	1.539(3)	C11-P1	1.861(2)
C15-C17	1.525(3)	C15-C18	1.532(3)
C15-C16	1.534(3)	C15-P2	1.864(2)
C19-C22	1.527(3)	C19-C21	1.529(3)
C19-C20	1.534(3)	C19-P2	1.863(2)
O1-P1	1.6520(14)	O2-P2	1.6534(13)
C1-Ni1-P1	81.31(6)	C1-Ni1-P2	81.56(6)
P1-Ni1-P2	162.81(2)	C1-Ni1-B1	179.30(9)
P1-Ni1-B1	99.15(7)	P2-Ni1-B1	98.00(7)
C2-C1-C6	114.39(16)	C2-C1-Ni1	122.73(14)
C6-C1-Ni1	122.88(14)	C3-C2-O2	118.53(17)
C3-C2-C1	124.06(18)	O2-C2-C1	117.41(16)
C2-C3-C4	118.43(18)	C3-C4-C5	120.80(17)
C6-C5-C4	118.16(18)	O1-C6-C5	118.53(17)
O1-C6-C1	117.30(16)	C5-C6-C1	124.17(18)
C9-C7-C10	109.35(18)	C9-C7-C8	108.60(19)
C10-C7-C8	108.76(18)	C9-C7-P1	113.26(14)
C10-C7-P1	111.76(15)	C8-C7-P1	104.91(14)
C13-C11-C14	109.66(19)	C13-C11-C12	109.93(19)
C14-C11-C12	107.81(19)	C13-C11-P1	111.18(15)
C14-C11-P1	104.65(15)	C12-C11-P1	113.40(16)
C17-C15-C18	110.42(19)	C17-C15-C16	107.7(2)
C18-C15-C16	108.40(19)	C17-C15-P2	113.48(14)
C18-C15-P2	112.09(15)	C16-C15-P2	104.32(14)
C22-C19-C21	108.8(2)	C22-C19-C20	108.6(2)
C21-C19-C20	109.3(2)	C22-C19-P2	104.89(16)
C21-C19-P2	111.82(15)	C20-C19-P2	113.18(16)

C6-O1-P1	112.69(12)	C2-O2-P2	112.63(11)
O1-P1-C7	99.32(8)	O1-P1-C11	100.22(8)
C7-P1-C11	114.01(10)	O1-P1-Ni1	105.75(5)
C7-P1-Ni1	118.17(7)	C11-P1-Ni1	115.58(7)
O2-P2-C19	99.42(8)	O2-P2-C15	99.42(8)
C19-P2-C15	114.28(9)	O2-P2-Ni1	105.59(5)
C19-P2-Ni1	117.64(7)	C15-P2-Ni1	116.40(7)

Table S4 Anisotropic atomic displacement parameters ($Å^2$) of [2,6-(^{t}Bu$_2$PO)$_2$C$_6$H$_3$]Ni((η^2-BH$_4$)
The anisotropic atomic displacement factor exponent takes the form: $-2\pi^2[\ h^2\ a^{*2}\ U_{11} + ... + 2\ h\ k\ a^*\ b^*\ U_{12}\ ]$

	U_{11}	U_{22}	U_{33}	U_{23}	U_{13}	U_{12}
Ni1	0.01122(13)	0.01168(13)	0.00789(11)	0.00342(8)	-0.00048(9)	0.00181(9)
B1	0.0208(12)	0.0195(12)	0.0170(10)	0.0096(9)	-0.0049(9)	-0.0012(10)
C1	0.0097(9)	0.0133(9)	0.0095(8)	0.0029(6)	0.0027(6)	0.0029(7)
C2	0.0130(9)	0.0096(8)	0.0083(7)	0.0019(6)	0.0030(7)	0.0031(7)
C3	0.0133(9)	0.0155(9)	0.0101(8)	0.0022(7)	-0.0003(7)	0.0024(7)
C4	0.0152(10)	0.0157(9)	0.0095(8)	0.0036(7)	-0.0019(7)	0.0039(8)
C5	0.0164(10)	0.0152(9)	0.0107(8)	0.0054(7)	-0.0006(7)	0.0026(8)
C6	0.0098(9)	0.0127(9)	0.0106(8)	0.0017(7)	-0.0001(7)	0.0010(7)
C7	0.0158(10)	0.0138(9)	0.0124(8)	0.0012(7)	0.0019(7)	0.0021(8)
C8	0.0212(12)	0.0242(12)	0.0291(12)	-0.0015(9)	0.0096(9)	0.0054(9)
C9	0.0305(13)	0.0143(10)	0.0241(11)	0.0041(8)	0.0068(9)	0.0014(9)
C10	0.0360(14)	0.0215(11)	0.0118(9)	-0.0020(8)	-0.0011(9)	0.0037(10)
C11	0.0127(10)	0.0233(11)	0.0162(9)	0.0085(8)	0.0050(7)	0.0047(8)
C12	0.0238(12)	0.0392(15)	0.0331(13)	0.0233(11)	0.0172(10)	0.0134(11)
C13	0.0122(10)	0.0320(13)	0.0276(11)	0.0112(10)	0.0000(9)	0.0055(9)
C14	0.0258(13)	0.0331(14)	0.0229(11)	0.0016(9)	0.0100(9)	0.0115(11)
C15	0.0142(10)	0.0147(9)	0.0105(8)	0.0020(7)	0.0026(7)	0.0012(7)
C16	0.0313(14)	0.0255(12)	0.0304(12)	0.0083(10)	0.0146(10)	0.0161(10)
C17	0.0301(14)	0.0286(14)	0.0287(12)	-0.0033(10)	0.0148(11)	-0.0115(11)
C18	0.0294(13)	0.0512(17)	0.0142(10)	0.0138(10)	0.0061(9)	0.0120(12)
C19	0.0216(11)	0.0139(9)	0.0147(9)	0.0023(7)	0.0025(8)	0.0096(8)
C20	0.0332(15)	0.0178(12)	0.0452(15)	-0.0123(10)	-0.0114(12)	0.0110(11)
C21	0.0454(16)	0.0263(13)	0.0270(12)	-0.0005(10)	-0.0137(11)	0.0228(12)
C22	0.072(2)	0.0428(18)	0.0565(19)	0.0235(15)	0.0483(18)	0.0398(17)
O1	0.0139(7)	0.0125(7)	0.0110(6)	0.0037(5)	-0.0028(5)	-0.0012(5)
O2	0.0161(7)	0.0087(6)	0.0098(6)	0.0036(5)	-0.0017(5)	0.0004(5)

P1	0.0100(2)	0.0127(2)	0.0085(2)	0.00313(17)	-0.00003(17)	0.00171(18)
P2	0.0130(2)	0.0099(2)	0.0078(2)	0.00216(16)	0.00063(17)	0.00343(18)

Table S5 Hydrogen atomic coordinates and isotropic atomic displacement parameters ($Å^2$) of [2,6-(^{t}Bu$_2$PO)$_2$C$_6$H$_3$]Ni((η^2-BH$_4$)

	x/a	y/b	z/c	U(eq)
H1B	0.295(3)	0.303(2)	0.1726(16)	0.022(7)
H2B	0.434(3)	0.221(2)	0.0926(18)	0.020(6)
H3B	0.209(4)	0.198(2)	0.043(2)	0.034(8)
H4B	0.352(4)	0.338(3)	0.048(2)	0.037(8)
H3	0.9327	0.4119	0.5259	0.016
H4	0.8620	0.2468	0.5987	0.016
H5	0.6232	0.0893	0.5232	0.017
H8A	0.5624	-0.0351	0.2268	0.038
H8B	0.5608	0.0381	0.1386	0.038
H8C	0.5163	-0.1015	0.1088	0.038
H9A	0.1150	-0.1686	0.1923	0.036
H9B	0.2860	-0.1506	0.2685	0.036
H9C	0.2598	-0.2233	0.1530	0.036
H10A	0.2484	-0.1152	0.0064	0.038
H10B	0.2804	0.0236	0.0333	0.038
H10C	0.1099	-0.0607	0.0552	0.038
H12A	-0.0543	0.0043	0.3845	0.042
H12B	0.1379	0.0051	0.4164	0.042
H12C	0.0258	-0.0833	0.3151	0.042
H13A	-0.0562	-0.0106	0.1639	0.036
H13B	0.0179	0.1235	0.1581	0.036
H13C	-0.1273	0.0874	0.2263	0.036
H14A	0.1673	0.2693	0.3245	0.04
H14B	0.2291	0.2218	0.4212	0.04
H14C	0.0329	0.2126	0.3922	0.04
H16A	0.7842	0.2620	0.1457	0.04
H16B	0.9367	0.3372	0.2348	0.04
H16C	0.9615	0.3286	0.1170	0.04
H17A	1.0607	0.5404	0.1583	0.05
H17B	1.0135	0.5554	0.2720	0.05
H17C	0.9377	0.6185	0.1911	0.05
H18A	0.7068	0.5056	0.0500	0.046

H18B	0.6405	0.3662	0.0322	0.046
H18C	0.8238	0.4269	0.0075	0.046
H20A	0.6828	0.7377	0.3628	0.053
H20B	0.8029	0.6981	0.2856	0.053
H20C	0.7975	0.6569	0.3925	0.053
H21A	0.4045	0.5170	0.1539	0.049
H21B	0.5728	0.6124	0.1432	0.049
H21C	0.4397	0.6508	0.2108	0.049
H22A	0.5200	0.5203	0.4199	0.072
H22B	0.3661	0.4707	0.3266	0.072
H22C	0.4211	0.6062	0.3818	0.072

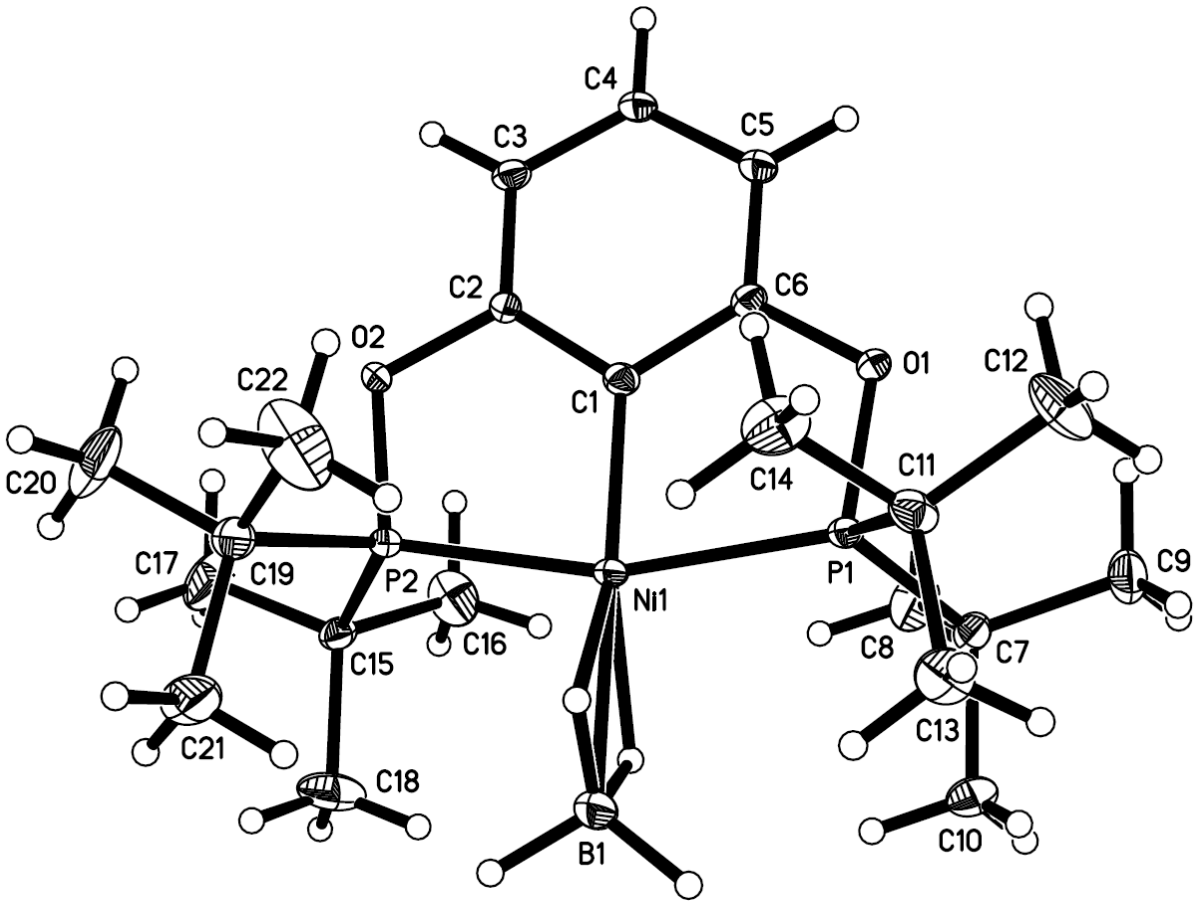

Figure S44 Thermal ellipsoid plots of [2,6-(^{t}Bu$_2$PO)$_2$C$_6$H$_3$]Ni(BH$_4$) at the 50 % probability level.

Table S6 Summary of crystal data and structure refinement for complexes **1c, 1d** and **2**

	1c	**1d**	**2**
Empirical formula	$C_{28}H_{44}NiO_2P_2S$	$C_{29}H_{43}F_3NiO_2P_2S$	$C_{29}H_{46}NiO_2P_2S$
Formula weight	565.34	633.32	579.37
Temp, K	153(2)	296(2)	103(2)
Crystal system	Triclinic	Monoclinic	Monoclinic
Space group	P -1	P 21/c	P 1 21/c 1
a, Å	8.5294(3)	11.1235(11)	19.7537(6)
b, Å	11.3723(4)	15.9839(15)	10.5331(3)
c, Å	16.2502(5)	18.1662(17)	15.3748(5)
α (°)	77.6151(19)	90	90
β (°)	80.615(2)	91.3393(11)	112.3046(17)
γ (°)	73.477(2)	90	90
Volume, Å^3	1467.20(9)	3229.0(5)	2959.65(16)
Z	2	4	4
d_{calc}, g cm^{-3}	1.280	1.286	1.300
λ, Å	0.71073	0.71073	0.71073
μ, mm^{-1}	0.864	0.805	0.858
No. of data collected	111732	25291	59906
No. of unique data	19630	7110	13126
R_{int}	0.0790	0.0252	0.0764
Goodness-of-fit on F^2	1.025	1.067	1.019
R_1, wR_2 ($I > 2\sigma(I)$)	0.0468, 0.0917	0.0446, 0.1174	0.0416, 0.0895
R_1, wR_2 (all data)	0.0967, 0.1092	0.0638, 0.1377	0.0676, 0.0999

Table S7 Summary of crystal data and structure refinement for complexes **1a**, **1b**, **4** and **6**

	1a	**1b**	**4**	**6**
Empirical formula	$C_{29}H_{46}NiO_3P_2S$	$C_{29}H_{46}NiO_2P_2S$	$C_{25}H_{38}NiO_2P_2S$	$C_{30}H_{39}BNiO_6P_2$
Formula weight	595.37	579.35	523.26	627.05
Temp, K	100(2)	296(2)	103(2)	293(2)
Crystal system	Triclinic	Monoclinic	Triclinic	Triclinic
Space group	P-1	P 21/n	P -1	P -1
a, Å	11.3208(8)	11.1532(14)	12.4676(7)	10.7701(9)
b, Å	16.0917(11)	19.273(2)	12.7321(7)	11.5716(14)
c, Å	27.9299(19)	15.5090(19)	16.5948(9)	14.5650(16)
α (°)	100.6840(10)	90	97.829(2)	72.803(10)
β (°)	100.6810(10)	110.332(2)	91.1728(19)	79.684(8)
γ (°)	103.9190(10)	90	91.620(2)	62.913(10)
Volume, Å^3	4711.3(6)	3126.0(6)	2607.9(2)	1541.7(3)
Z	6	4	4	2
d_{calc}, g cm^{-3}	1.259	1.231	1.333	1.351
λ, Å	0.71073	0.71073	0.71073	0.71073
μ, mm^{-1}	0.813	0.812	0.966	0.773
No. of data collected	33145	18682	123122	12939
No. of unique data	16577	7428	21852	8120
R_{int}	0.0240	0.0369	0.1207	0.0295
Goodness-of-fit on F^2	1.074	1.041	1.005	1.043
R_1, wR_2 ($I > 2\sigma(I)$)	0.0387, 0.0991	0.0374, 0.0848	0.0501, 0.0947	0.0443, 0.0918
R_1, wR_2 (all data)	0.0655, 0.1273	0.0564, 0.0938	0.1055, 0.1161	0.0601, 0.1007

Table S8 Selected bond length (Å) and angles (˚) for complexes **1a**-**d**, **2**, **4** and **6**

1a	**1b**	**1c**	**1d**	**2**	**4**	**6**
Ni2-C30, 1.899(3)	Ni1-C6, 1.907(2)	Ni1-C1, 1.8998(11)	Ni1-C7, 1.898(3)	Ni1-C1, 1.8989(13)	Ni1-C1, 1.8995(19)	Ni1-C2, 1.880(2)
Ni2-P3, 2.1955(8)	Ni1-P1, 2.1974(6)	Ni1-P1, 2.1750(3)	Ni1-P1, 2.2103(8)	Ni1-P1, 2.1674(4)	Ni1-P1, 2.1356(6)	Ni1-P1, 2.2108(7)
Ni2-P4, 2.2024(8)	Ni1-P2, 2.1899(6)	Ni1-P2, 2.2160(3)	Ni1-P2, 2.1963(8)	Ni1-P2, 2.2103(4)	Ni1-P2, 2.1589(6)	Ni1-P2, 2.1999(7)
Ni2-S2, 2.2556(9)	Ni1-S1, 2.2282(6)	Ni1-S1, 2.2241(3)	Ni1-S1, 2.2422(8)	Ni1-S1, 2.2088(4)	Ni1-S1, 2.2010(6)	Ni1-O1, 1.9660(15)
C52-S2, 1.760(3)	C19-S1, 1.773(2)	C23-S1, 1.7633(12)	C1-S1, 1.741(3)	C23-S1, 1.8208(15)	C19-S1, 1.831(2)	O1-B1, 1.548(3)
P3-Ni2-P4, 163.04(3)	P1-Ni1-P2, 163.46(2)	P1-Ni1-P2, 163.811(13)	P1-Ni1-P2, 163.07(3)	P1-Ni1-P2, 163.143(16)	P1-Ni1-P2, 163.25(2)	P1-Ni1-P2, 160.55(3)
S2-Ni2-C30, 173.38(9)	S1-Ni1-C6, 170.84(7)	S1-Ni1-C1, 166.65(4)	S1-Ni1-C7, 171.67(8)	S1-Ni1-C1, 168.62(4)	S1-Ni1-C1, 169.79(6)	O1-Ni1-C2, 173.71(8)
P3-Ni2-S2, 97.13(4)	P1-Ni1-S1, 103.58(2)	P1-Ni1-S1, 90.672(12)	P1-Ni1-S1, 99.87(3)	P1-Ni1-S1, 90.504(15)	P1-Ni1-S1, 90.71(2)	P1-Ni1-O1, 99.55(5)
P4-Ni2-S2, 98.93(4)	P2-Ni1-S1, 92.85(2)	P2-Ni1-S1, 105.359(13)	P2-Ni1-S1, 96.18(3)	P2-Ni1-S1, 106.353(15)	P2-Ni1-S1, 105.94(2)	P2-Ni1-O1, 98.24(5)
Ni2-S2-C52, 113.42(11)	Ni1-S1-C19, 117.75(7)	Ni1-S1-C23, 115.49(4)	Ni1-S1-C1, 115.46(10)	Ni1-S1-C23, 111.56(5)	Ni1-S1-C19, 111.12(7)	Ni1-O1-B1, 129.22(14)